50. Liu JH, Li HW, Tong M et al (2004) Genetic risk factors of prostate cancer in Han nationality population in Northern China and a preliminary study of the reason of racial difference in prevalence of prostate cancer. Zhonghua Yi Xue Za Zhi 84(5):364–368
51. Huang SP, Chou YH, Wayne Chang WS et al (2004) Association between vitamin D receptor polymorphisms and prostate cancer risk in a Taiwanese population. Cancer Lett 207(1):69–77
52. Nam RK, Zhang WW, Trachtenberg J et al (2003) Comprehensive assessment of candidate genes and serological markers for the detection of prostate cancer. Cancer Epidemiol Biomarkers Prev 12(12):1429–1437
53. Tayeb MT, Clark C, Haites NE et al (2003) CYP3A4 and VDR gene polymorphisms and the risk of prostate cancer in men with benign prostate hyperplasia. Br J Cancer 88(6):928–932
54. Bodiwala D, Luscombe CJ, French ME et al (2004) Polymorphisms in the vitamin D receptor gene, ultraviolet radiation, and susceptibility to prostate cancer. Environ Mol Mutagen 43(2):121–127
55. Cheteri MB, Stanford JL, Friedrichsen DM et al (2004) Vitamin D receptor gene polymorphisms and prostate cancer risk. Prostate 59(4):409–418
56. Gsur A, Madersbacher S, Haidinger G et al (2002) Vitamin D receptor gene polymorphism and prostate cancer risk. Prostate 51(1):30–34

Lack of Involvement of the *GNAS1* T393C Polymorphism in Prostate Cancer Risk in a Japanese Population

MASATOSHI WATANABE[1,2], YOSHIFUMI HIROKAWA[1], MAYUMI TSUJI[3], MAKOTO YANAGAWA[4], TETSUYA MURATA[5], HIROYOSHI SUZUKI[6], TOMOHIKO ICHIKAWA[6], TAKAHIKO KATOH[3], YOSHIKI SUGIMURA[7] and TAIZO SHIRAISHI[1]

[1]Department of Pathologic Oncology, Institute of Molecular and Experimental Medicine and [7]Division of Nephro-Urologic Surgery and Andrology, Department of Reparative and Regenerative Medicine, Mie University Graduate School of Medicine, 2-174 Edobashi, Tsu; [2]Laboratory for Medical Engineering, Division of Materials Science and Chemical Engineering, Graduate School of Engineering, Yokohama National University, Yokohama; [3]Department of Public Health, Graduate School of Medical Sciences, Kumamoto University, Kumamoto; [4]Department of Urology, Matsusaka Saiseikai General Hospital, Matsusaka; [5]Department of Pathology, JA Suzuka General Hospital, Suzuka; [6]Department of Urology, Graduate School of Medicine, Chiba University, Chiba, Japan

Abstract. *Background: GNAS1 encodes the α-subunit of the G_s protein ($G_{s\alpha}$), which binds GTP and stimulates adenylyl cyclase. Activating mutations lead to somatotroph, thyroid, adrenal and gonadal adenomas or the McCune-Albright syndrome and recently the T399C polymorphism in GNAS1 has been reported to be associated with malignancies. The purpose of the present case-control study with 349 Japanese prostate cancer patients and 203 urological controls was to determine whether the GNAS1 T393C polymorphism is associated with prostate cancer risk. Materials and Methods: The GNAS1 T393C polymorphism was examined by polymerase chain reaction-restriction fragment length polymorphism (PCR-RFLP) analysis. Odds ratios (OR) were adjusted for age using multiple logistic regression analysis with SPSS Medical Pack. Results: The allele frequencies were compatible with the control population in Hardy-Weinberg equilibrium with 80, 169 and 100 for GNAS1 C/C, C/T and T/T, respectively in the patients with prostate cancer, compared with 42, 94 and 67 in the controls. No association between the GNAS1 polymorphism and prostate cancer risk was apparent. The C/C genotype was more frequent among the prostate cancer patients (22.9%) than the controls (20.7%), although without significance (OR, 1.30; 95% CI, 0.80-2.12; p=0.29). Conclusion: This pilot study does not support involvement of the GNAS1 polymorphism in prostate cancer risk.*

Correspondence to: Taizo Shiraishi, MD, Ph.D., Department of Pathologic Oncology, Institute of Molecular and Experimental Medicine, Mie University Graduate School of Medicine, 2-174 Edobashi, Tsu, Japan. Tel/Fax: +81 592315210, e-mail; tao@doc.medic. mie-u.ac.jp

Key Words: GNAS1, polymorphism, prostate cancer.

Prostate cancer is one of the most common male malignancies in industrialized nations and its incidence is generally rising (1). Both genetic and environmental influences may be involved in its etiology (2), including ethnic background, family history, smoking, and diet. Some epidemiological studies have supported an association between dietary fat, particularly saturated or animal , and prostate cancer risk (2, 3). Ethnicity, which reflects the shared genetic inheritance within a group, is clearly an important factor in determining the risk of prostate cancer (2, 4). Although it is well-known that the incidence of prostate cancer is still 2- to 3-fold higher in American Caucasians than in Asians, the numbers of clinical cases have been increasing yearly in Japan and in 2020 prostate cancer is expected to be the most common male neoplasm, as was the case for the stomach in 1995 (4, 5). In addition, a familial aggregation is evident, and men with a family history of prostate cancer have a 2-to 3-fold higher incidence than the general population (2). Such an influence of inheritance of genes may reflect relatively high penetrance, but most cases involve polymorphisms with low penetrance.

Genetic polymorphisms affecting a number of metabolic enzymes have been found to modulate prostate cancer risk (2, 6-8). The most studied polymorphisms are in steroid hormone-related genes such as the androgen receptor, 5 α-reductase type II (SRD5A2) and cytochrome P450c17α

(CYP17) (6, 7). There is evidence for a hormonal etiology of prostate cancer involving the action of androgens, required for differentiation and growth of the prostate. Testosterone is synthesized from cholesterol by a series of enzymatic reactions involving CYP17 and is then converted to dihydrotestosterone (DHT) in the prostate by SRD5A2. DHT binds to the androgen receptor (AR), leading to the transactivation of some genes with AR-responsive elements. An improved understanding of the molecular epidemiology of prostate cancer should help define the relevance of new prognostic indices and aid treatment decisions.

Heterotrimeric guanine nucleotide-binding proteins (G proteins), which couple seven transmembrane receptors to adenylyl cyclase and mediate signal transduction across the cell membranes, are composed of three distinct subunits α, β, and γ which are encoded by separate genes (9-11). G proteins are generally defined by their specific α-subunit and are classified into four major classes (G_S, $G_{i/o}$, $G_{q/11}$ and $G_{12/13}$) based on amino acid substitution similarities of the α-subunits (10). The stimultory G protein (Gs) is expressed ubiquitously, being required for the activation of adenylyl cyclase and the generation of cyclic adenosine monophosphate (cAMP) in cells, *e.g.* pituitary target cells, in response to several hormones, such as growth hormone-releasing hormone (GHRH) and corticotroph-releasing hormone (CRH). The *GNAS1* gene, being located on chromosome 20q13.3, is a complex locus encoding multiple overlapping transcripts (9). Of these, the α subunit of the G_s ($G_{s\alpha}$) is the most extensively characterized and clinically relevant. Mutations of *GNAS1* may cause either loss or gain of function by inactivating or activating signal transduction, thus leading to the clinical phenotype of either hormone deficiency or excess (9). Inactivating germ-line mutations cause Albright's hereditary osteodystrophy (AHO) andpseudohypoparathyroidism (PHP), while activating mutations lead to somatotroph, thyroid, adrenal and gonadal adenomas or McCune-Albright syndrome (MAS) (9). MAS is classified by the triad of polyostoic fibrous dysplasia, hyperpigmented (café-au-lait) skin lesions, and gonadotropin-independent sexual precocity (12). In particular, amino acid substitutions replacing either Arg 201 or Gln 227 have been identified in a subset of growth hormone (GH)-secreting adenomas characterized by extremely high adenylyl cyclase activity and cAMP levels (13). $G_{s\alpha}$ appears to be the product of a proto-oncogene that is converted into an oncogene, designated *gsp*. However, few McCune-Albright syndrome patients have been reported to have a malignancy (12, 14-16). There is a common silent polymorphism T393C in exon 5 of *GNAS1*, which has been studied in Caucasians and Japanese in relation to hypertension (17-20). Associations with other diseases, including malignancy, have also been reported (21-30).

In the present study, the prevalence of the T393C polymorphism of *GNAS1* in patients with prostate cancer and benign prostatic hyperplasia (BPH) controls were examined to evaluate its influence on the risk of prostate cancer.

Table I. *Clinicopathological data.*

	Patients	Controls	*p*-Value
N	349	203	
Mean age	68.7±7.1	70.6±7.4	0.34
Histology			
P	59 (17.3)		
M	145 (42.3)		
W	138 (40.4)		
Stage			
A or B	212 (60.7)		
C	85 (24.4)		
D	52 (14.9)		
GS			
<5	9 (3.6)		
6	47 (19.1)		
7	149 (60.6)		
8-10	41 (16.7)		
PSA level (ng/ml)			
<4	7 (4.8)		
4-10	72 (49.0)		
10-20	45 (30.6)		
20-50	20 (13.6)		
50<	3 (2.0)		

P: Poorly differentiated adenocarcinoma; M: moderately differentiated adenocarcinoma; W: well-differentiated adenocarcinoma; GS: Gleason score; PSA: prostatic-specific antigen; Stage: A (T_{1a-b}, N_0, M_0), B (T_{1c-2}, N_0, M_0), C (T_{3-4}, N_0, M_0), D ($T_{1-4}N_1M_{0-1}$ or $T_{1-4}N_{0-1}M_1$).

Materials and Methods

Selection of patients and controls. Data for prostate cancer subjects (n=349) and controls (n=203) were collected from the records of the Departments of Urology at Mie University Hospital, Chiba University Hospital, JA Suzuka Central General Hospital and Matsusaka Saiseikai Hospital between 1991 and 2007. All were Japanese men and the prostate cancer patients were all histologically confirmed and characterized in terms of their clinical staging (Tumor-Node-Metastasis system) and grading (The General Rules for Clinical and Pathological Studies on Prostate cancer, 2001 established by the Japanese Urological Association and the Japanese Society of Pathology). The cancer cases were classified as stage A ($T_{1a-b}N_0M_0$), stage B ($T_{1c-2}N_0M_0$), stage C ($T_{3-4}N_0M_0$) or stage D ($T_{1-4}N_1M_{0-1}$ or $T_{1-4}N_{0-1}M_1$) based on the modified Whitmore-Jewett system. One hundred and thirty eight patients (40.4%) had well-differentiated, 145 (42.3%) moderately differentiated and 59 (17.3%) poorly differentiated adenocarcinomas. Regarding clinical staging, 212 (60.7%) were in stage A or B, 85 (24.4%) were in stage C and 52 (14.9%) were in stage D. The control group was composed of BPH patients who were healthy and confirmed to be free of prostate cancer by no elevation of serum PSA and/or a negative biopsy. Retropubic prostatectomy was performed for 99 of the controls, with pathological examination to exclude the presence of prostate cancer. All gave informed consent to participate in this molecular genetic study of prostate cancer. The Ethical Committee of Mie University approved this study. The clinicopathological profiles of the study participants are shown in Table I.

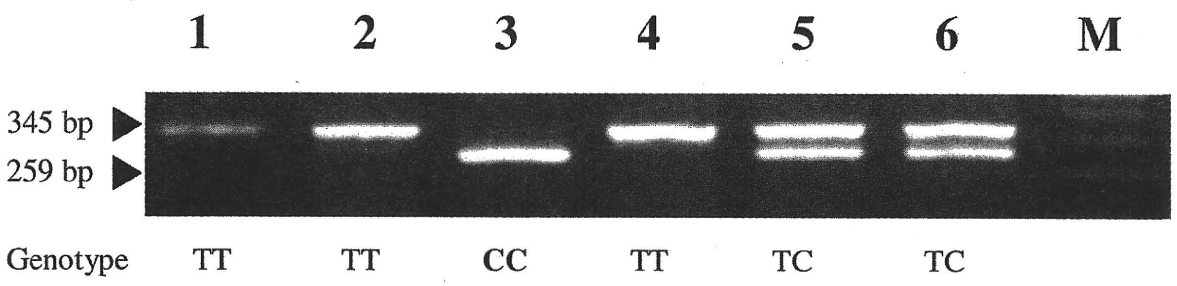

Figure 1. *Representative RFLP patterns of GNAS1 polymorphisms in prostate cancer cases.*

DNA extraction. DNA was isolated from the peripheral blood of all the prostate cancer patients and 104 controls and from the frozen prostate tissue in 99 controls (6).

Genotyping of GNAS1. Genotyping was performed by the polymerase chain reaction-restriction fragment length polymorphism (PCR-RFLP) method. For *GNAS1* T393C, the primers 5'-CTCCTAACTGACA TGGTGCAA-3' and 5'-TAAGGCCACACAA GTCGGGT-3' were used. The PCR products were digested with the restriction enzyme *Fok* I (the T allele produces a 345-bp band; the C allele produces 259- and 86-bp bands). Thus, the unrestricted products (345 bp) represent the TT genotype; the completely restricted products (259 and 86 bp) represent the CC genotype (Figure 1) (29).

Statistical analysis. To examine associations between genotypes and the development of prostate cancer, the odds ratios (ORs) and confidence intervals (CI) were calculated. The ORs were adjusted for age using multiple logistic regression analysis with Dr.SPSS (the Statistical Program for Social Sciences) II for Windows (SPSS, Tokyo).

Results

The mean age of the prostate cancer patients at diagnosis was 68.7±7.1 years and of the controls, 70.6±7.4 years. Although the mean age of the patients was thus lower than the controls, the difference was not significant (p=0.34). The data for the genotypes of the *GNAS1* gene in the prostate cancer patients and controls and their relationships to risk among Japanese males are shown in Table II. The allele frequencies of the *GNAS1* polymorphisms in the patients and controls were compatible with Hardy-Weinberg equilibrium distribution (p>0.05). The frequencies of the *GNAS1* CC, CT and TT genotypes were 22.9%, 48.4% and 28.7% in the prostate cancer patients, compared with 20.7%, 46.3% and 33.0% in the controls. No association between the *GNAS1* CC genotype and prostate cancer risk was apparent (OR 1.30; 95% CI, 0.80-2.12; p=0.29). The OR for prostate cancer risk for men with the CT and CC genotypes was 1.21 (95% CI, 0.81-1.77; p=0.32).

The relationships between the *GNAS1* T393C genotypes and the clinicopathological factors, including histology, staging, Gleason score and serum PSA were investigated (Table III). There was no statistically significant association of the *GNAS1* genotypes with these factors.

Table II. *GNAS1 genotype distribution in patients with prostate cancer and controls.*

Genotype	Patients with prostate cancer	Controls	OR (95% CI)	p-Value
TT	100 (28.7%)	67 (33.0%)	1.00 (referent)	
CT	169 (48.4%)	94 (46.3%)	1.17 (0.78-1.75)	0.45
CC	80 (22.9%)	42 (20.7%)	1.30 (0.80-2.12)	0.29
CT+CC	249 (71.3%)	136 (67.0%)	1.21 (0.83-1.77)	0.32

Results of logistic regression analyses. Age was always included in the models as a covariate.

Discussion

The T393C polymorphism of *GNAS1* is associated with altered $G_{s\alpha}$ mRNA expression in different tissues (21). The T to C substitution at position 393 changes the mRNA folding structures (22), so that genotype-dependent differences in mRNA decay due to an altered secondary structure could be the cause of the variation in $G_{s\alpha}$ mRNA expression (23, 24). *In vitro* studies suggested that increased expression of $G_{s\alpha}$ is associated with enhanced apoptosis and that a second messenger, cAMP, which functions downstream of the G proteins, plays a major role in proapoptotic processes (26, 28, 29). With the reported risk of malignancy, the focus has been on the homozygous CC or TT genotypes. Bladder cancer, colorectal cancer, clear cell renal cell carcinoma, chronic lymphocytic leukemia and squamous cell carcinoma patients with a homozygous CC genotype appear to be at the highest risk of progression, metastasis or tumor-related death, while intrahepatic cholangiocarcinoma and breast carcinoma patients with a homozygous TT genotype showed similar results. In the present preliminary study, the CC genotype was more frequent in the prostate cancer cases, but this was not significant (OR=1.30; 95% CI, 0.80-2.12; p=0.29).

Table III. *Clinicopathological factors and GNAS1 genotype in a Japanese population.*

Genotype	TT / CC	OR (95% CI)	TT / CT+CC	OR (95% CI)
Histology				
P	20/11	1.00 (referent)	20/39	1.00 (referent)
M	38/36	1.73 (0.73-4.12)	38/107	1.44 (0.75-2.76)
W	40/30	1.39 (0.58-3.36)	40/98	1.22 (0.64-2.36)
	p for trend=0.445		*p* for trend=0.550	
Stage				
A or B	57/51	1.00 (reference)	57/155	1.00 (referent)
C	29/14	0.53 (0.25-1.12)	29/56	0.72 (0.42-1.25)
D	14/15	1.16 (0.50-2.68)	14/38	1.06 (0.53-2.12)
	p for trend=0.175		*p* for trend=0.462	
GS				
8-10	14/6	1.00 (referent)	14/27	1.00 (referent)
7	42/36	2.05 (0.71-5.93)	42/107	1.27 (0.61-2.67)
6	12/8	1.60 (0.43-6.01)	12/35	1.44 (0.57-3.64)
<5	2/2	2.33 (0.26-20.67)	2/7	1.85 (0.34-10.13)
	p for trend= 0.578		*p* for trend=0.456	
PSA				
<4	4/1	1.00 (referent)	4/3	1.00 (referent)
4-10	17/16	3.85 (0.37-40.38)	17/55	3.87 (0.77-19.46)
10-20	13/9	2.85 (0.25-32.32)	13/32	2.96 (0.57-15.42)
20-50	5/5	4.08 (0.32-52.50)	5/15	3.62 (0.58-22.47)
50<	3/0	-	3/0	-
	p for trend=0.238		*p* for trend=0.048	

P: Poorly differentiated adenocarcinoma; M: moderately differentiated adenocarcinoma; W: well-differentiated adenocarcinoma; GS: Gleason score; PSA: prostatic-specific antigen; Stage: A (T_{1a-b}, N_0, M_0), B (T_{1c-2}, N_0, M_0), C (T_{3-4}, N_0, M_0), D ($T_{1-4}N_1M_{0-1}$ or $T_{1-4}N_{0-1}M_1$).

cAMP has been shown to induce a mitogenic response or increase *in vitro* invasiveness in LNCaP prostate cancer cells (31, 32). It has also been reported that persistent activation of Gsα-mediated signaling stimulates the proliferation of certain cell types and can contribute to invasive tumor development in humans (33), also changing the proliferative, invasive and tumorigenic properties of PC-3M prostate cancer cells (34, 35). In the clinic, progression of prostate cancer to a hormone-refractory state is a critical problem. The mechanisms are complex and include both the selection and outgrowth of pre-exisiting clones of androgen-independent cells as well as adaptive up-regulation of genes that predispose cancer cells to survive and grow after androgen ablation, but are still not completely understood. Kasbohm *et al.* demonstrated that the up-regulation of a subunit of heterotrimeric guanine nucleotide-binding Gs protein activated the AR in prostate cancer cells, synergizing with low concentration of androgen (36). Bagchi *et al.* detected cAMP-dependent protein kinase A (PKA) activation in both androgen-dependent (LNCaP and LAPC4) and androgen-independent (PC3M) prostate cancer cells and established generality for the pathway (37). They concluded that androgen might evoke a nongenomic signaling pathway to activate cAMP-dependent PKA which is needed for the genomic functioning of nuclear AR. Thus, persistant stimulation of $G_{s\alpha}$-mediated signaling could accelerate prostate tumor growth and the formation of metastases and offer a target for treatment. However, no correlations between clinicopathological factors and this polymorphism were detected in the present study. Further investigation of clinical data including relapse period and clinical outcome should however be performed.

The G_{12} subfamily of heterotrimeric G proteins has been of interest to cancer researchers because its members were found to promote the growth and oncogenic transformation of murine fibroblasts (38). The G_{12} subfamily has been shown to promote prostate and breast cancer cell invasion *in vitro* (39, 40) and were also reported to be regulators of lysophosphatidic acid-induced ovarian cancer cell migration *in vitro* (41). These studies suggested that G_{12} subfamily-induced Rho activation may be critical for cancer cell behavior. Further studies of other G protein subfamilies including these polymorphisms should be conducted.

In conclusion, the present investigation did not provide support for a contribution of the *GNAS1* polymorphism to the risk of prostate cancer in this Japanese population.

Acknowledgements

This study was supported in part by a Grant-in-Aid for Cancer Research from the Ministry of Health, Labour and Welfare of Japan,

and by a Grant-in-Aid for Scientific Research on Priority Areas of Cancer from the Ministry of Education, Culture, Sport, Science and Technology of Japan.

References

1 Parkin DM, Bray F, Ferlay J and Pisani P: Global cancer statistics, 2002. CA Cancer J Clin *55*: 74-108, 2005.

2 Bostwick DG, Burke HB, Djakiew D, Euling S, Ho SM, Landolph J, Morrison H, Sonawane B, Shifflett T, Waters DJ and Timms B: Human prostate cancer risk factors. Cancer *101(10 Suppl)*: 2371-2490, 2004.

3 Stacewicz-Sapuntzakis M, Borthakur G, Burns JL and Bowen PE: Correlations of dietary patterns with prostate health. Mol Nutr Food Res *52*: 114-130, 2008.

4 Watanabe M, Nakayama T, Shiraishi T, Stemmermann GN and Yatani R: Comparative studies of prostate cancer in Japan *versus* the United States. A review. Urol Oncol *5*: 274-283, 2000.

5 Tabata N, Ohno Y, Matsui R, Sugiyama H, Ito Y, Tsukuma H and Oshima A: Partial cancer prevalence in Japan up to 2020: estimates based on incidence and survival data from population-based cancer registries. Jpn J Clin Oncol *38*: 146-157, 2008.

6 Yamada Y, Watanabe M, Murata M, Yamanaka M, Kubota Y, Ito H, Katoh T, Kawamura J, Yatani R and Shiraishi T: Impact of genetic polymorphisms of 17-hydroxylase cytochrome P-450 (CYP17) and steroid 5 alpha-reductase type II (SRD5A2) genes on prostate-cancer risk among the Japanese population. Int J Cancer *92*: 683-686, 2001.

7 Platz EA and Giovannucci E: The epidemiology of sex steroid hormones and their signaling and metabolic pathways in the etiology of prostate cancer. J Steroid Biochem Mol Biol *92*: 237-253, 2004.

8 Katoh T, Yamano Y, Tsuji M and Watanabe M: Genetic polymorphisms of human cytosol glutathione *S*-transferases and prostate cancer. Pharmacogenomics *9*: 93-104, 2008.

9 Weinstein LS, Yu S, Warner DR and Liu J: Endocrine manifestations of stimulatory G protein alpha-subunit mutations and the role of genomic imprinting. Endocr Rev *22*: 675-705, 2001.

10 Weinstein LS, Chen M, Xie T and Liu J: Genetic diseases associated with heterotrimeric G proteins. Trends Pharmacol Sci *27*: 260-266, 2006.

11 Koelle MR: Heterotrimeric G protein signaling: getting inside the cell. Cell *126*: 25-27, 2006.

12 Chanson P, Salenave S and Orcel P: McCune-Albright syndrome in adulthood. Pediatr Endocrinol Rev *4(Suppl 4)*: 453-462, 2007.

13 Lania A, Mantovani G and Spada A: Genetics of pituitary tumors: focus on G-protein mutations. Exp Biol Med (Maywood) *228*: 1004-1017, 2003.

14 Tanabeu Y, Nakahara S, Mitsuyama S, Ono M and Toyoshima S: Breast cancer in a patient with McCune-Albright syndrome. Breast Cancer *5*: 175-178, 1998.

15 Huston TL and Simmons RM: Ductal carcinoma *in situ* in a 27-year-old woman with McCune-Albright syndrome. Breast J *10*: 440-442, 2004.

16 Congedo V and Celi FS: Thyroid disease in patients with McCune-Albright syndrome. Pediatr Endocrinol Rev *4(Suppl 4)*: 429-433, 2007.

17 Jia H, Hingorani AD, Sharma P, Hopper R, Dickerson C, Trutwein D, Lloyd DD and Brown MJ: Association of the G(s)alpha gene with essential hypertension and response to beta-blockade. Hypertension *34*: 8-14, 1999.

18 Abe M, Nakura J, Yamamoto M, Jin JJ, Wu Z, Tabara Y, Yamamoto Y, Igase M, Kohara K and Miki T: Association of *GNAS1* gene variant with hypertension depending on smoking status. Hypertension *40*: 261-265, 2002.

19 Chen Y, Nakura J, Jin JJ, Wu Z, Yamamoto M, Abe M, Tabara Y, Yamamoto Y, Igase M, Bo X, Kohara K and Miki T: Association of the *GNAS1* gene variant with hypertension is dependent on alcohol consumption. Hypertens Res *26*: 439-444, 2003.

20 Yamamoto M, Abe M, Jin JJ, Wu Z, Tabara Y, Mogi M, Kohara K, Miki T and Nakura J: Association of a *GNAS1* gene variant with hypertension and diabetes mellitus. Hypertens Res *27*: 919-924, 2004.

21 Frey UH, Eisenhardt A, Lümmen G, Rübben H, Jöckel KH, Schmid KW and Siffert W: The T393C polymorphism of the G alpha s gene (*GNAS1*) is a novel prognostic marker in bladder cancer. Cancer Epidemiol Biomarkers Prev *14*: 871-877, 2005.

22 Frey UH, Alakus H, Wohlschlaeger J, Schmitz KJ, Winde G, van Calker HG, Jöckel KH, Siffert W and Schmid KW: *GNAS1* T393C polymorphism and survival in patients with sporadic colorectal cancer. Clin Cancer Res *11*: 5071-5077, 2005.

23 Frey UH, Lümmen G, Jäger T, Jöckel KH, Schmid KW, Rübben H, Müller N, Siffert W and Eisenhardt A: The *GNAS1* T393C polymorphism predicts survival in patients with clear cell renal cell carcinoma. Clin Cancer Res *12*: 759-763, 2006.

24 Frey UH, Nückel H, Sellmann L, Siemer D, Küppers R, Dürig J, Dührsen U and Siffert W: The *GNAS1* T393C polymorphism is associated with disease progression and survival in chronic lymphocytic leukemia. Clin Cancer Res *12*: 5686-5689, 2006.

25 Hahn S, Frey UH, Siffert W, Tan S, Mann K and Janssen OE: The CC genotype of the *GNAS* T393C polymorphism is associated with obesity and insulin resistance in women with polycystic ovary syndrome. Eur J Endocrinol *155*: 763-770, 2006.

26 Schmitz KJ, Lang H, Frey UH, Sotiropoulos GC, Wohlschlaeger J, Reis H, Takeda A, Siffert W, Schmid KW and Baba HA: *GNAS1* T393C polymorphism is associated with clinical course in patients with intrahepatic cholangiocarcinoma. Neoplasia *9*: 159-165, 2007.

27 Minoretti P, Politi P, Coen E, Di Vito C, Bertona M, Bianchi M and Emanuele E: The T393C polymorphism of the *GNAS1* gene is associated with deficit schizophrenia in an Italian population sample. Neurosci Lett *397*: 159-163, 2006.

28 Otterbach F, Callies R, Frey UH, Schmitz KJ, Wreczycki C, Kimmig R, Siffert W and Schmid KW: The T393C polymorphism in the gene *GNAS1* of G protein is associated with survival of patients with invasive breast carcinoma. Breast Cancer Res Treat *105*: 311-317, 2007.

29 Lehnerdt GF, Franz P, Zaqoul A, Schmitz KJ, Grehl S, Lang S, Schmid KW, Siffert W, Jahnke K and Frey UH: Overall and relapse-free survival in oropharyngeal and hypopharyngeal squamous cell carcinoma are associated with genotypes of T393C polymorphism of the *GNAS1* gene. Clin Cancer Res *4*: 1753-1758, 2008.

30 Kaderi MA, Murray F, Jansson M, Merup M, Karlsson K, Roos G, Aleskog A and Tobin G: The *GNAS1* T393C polymorphism and lack of clinical prognostic value in chronic lymphocytic leukemia. Leuk Res *32*: 984-987, 2008.

31 Shah GV, Rayford W, Noble MJ, Austenfeld M, Weigel J, Vamos S and Mebust WK: Calcitonin stimulates growth of human prostate cancer cells through receptor-mediated increase in cyclic adenosine 3',5'-monophosphates and cytoplasmic Ca2+ transients. Endocrinology *134*: 596-602, 1994.

32 Ritchie CK, Thomas KG, Andrews LR, Tindall DJ and Fitzpatrick LA: Effects of the calciotrophic peptides calcitonin and parathyroid hormone on prostate cancer growth and chemotaxis. Prostate *30*: 183-187, 1997.

33 Régnauld K, Nguyen QD, Vakaet L, Bruyneel E, Launay JM, Endo T, Mareel M, Gespach C and Emami S: G-protein alpha(olf) subunit promotes cellular invasion, survival, and neuroendocrine differentiation in digestive and urogenital epithelial cells. Oncogene *21*: 4020-4031, 2002.

34 Chien J, Wong E, Nikes E, Noble MJ, Pantazis CG and Shah GV: Constitutive activation of stimulatory guanine nucleotide binding protein (G(S)alphaQL)-mediated signaling increases invasiveness and tumorigenicity of PC-3M prostate cancer cells. Oncogene *18*: 3376-3382, 1999.

35 Chien J and Shah GV: Role of stimulatory guanine nucleotide binding protein (GSalpha) in proliferation of PC-3M prostate cancer cells. Int J Cancer *91*: 46-54, 2001.

36 Kasbohm EA, Guo R, Yowell CW, Bagchi G, Kelly P, Arora P, Casey PJ and Daaka Y: Androgen receptor activation by G(s) signaling in prostate cancer cells. J Biol Chem *280*: 11583-11589, 2005.

37 Bagchi G, Wu J, French J, Kim J, Moniri NH and Daaka Y: Androgens transduce the G alpha S-mediated activation of protein kinase A in prostate cells. Cancer Res *68*: 3225-3231, 2008.

38 Kelly P, Casey PJ and Meigs TE: Biologic functions of the G12 subfamily of heterotrimeric G proteins: growth, migration, and metastasis. Biochemistry *46*: 6677-6687, 2007.

39 Kelly P, Moeller BJ, Juneja J, Booden MA, Der CJ, Daaka Y, Dewhirst MW, Fields TA and Casey PJ: The G12 family of heterotrimeric G proteins promotes breast cancer invasion and metastasis. Proc Natl Acad Sci USA *103*: 8173-8178, 2006.

40 Kelly P, Stemmle LN, Medden JF, Fields TA, Daaka Y and Casey PJ: A role of the G12 family of heterotrimeric G proteins in prostate cancer invasion. J Biol Chem *281*: 26483-26490, 2006.

41 Bian D, Mahanivong C, Yu J, Frisch SM, Pan ZK, Ye RD and Huang S: The G12/13-RhoA signaling pathway contributes to efficient lysophosphatidic acid-stimulated cell migration. Oncogene *25*: 2234-2244, 2006.

Received July 5, 2008
Revised September 9, 2008
Accepted October 7, 2008

Mutation Research 654 (2008) 138–144

Contents lists available at ScienceDirect

Mutation Research/Genetic Toxicology and Environmental Mutagenesis

journal homepage: www.elsevier.com/locate/gentox
Community address: www.elsevier.com/locate/mutres

8-Hydroxydeoxyguanosine generated in the earthworm *Eisenia fetida* grown in metal-containing soil

Tamiji Nakashima[a], Toshihiro Okada[b], Junpei Asahi[c], Akihisa Yamashita[c], Kazuaki Kawai[d], Hiroshi Kasai[d], Koji Matsuno[e], Shinobu Gamou[f], Takeshi Hirano[c,*]

[a] *Department of Anatomy, School of Medicine, University of Occupational and Environmental Health, Japan, 1-1 Iseigaoka, Yahatanishi-ku, Kitakyushu, Fukuoka 807-8555, Japan*
[b] *Department of Chemical Processes and Environments, Faculty of Environmental Engineering, The University of Kitakyushu, 1-1 Hibikino, Wakamatsu-ku, Kitakyushu, Fukuoka 808-0135, Japan*
[c] *Graduate School of Environmental Engineering, University of Kitakyushu, 1-1 Hibikino, Wakamatsu-ku, Kitakyushu, Fukuoka 808-0135, Japan*
[d] *Department of Environmental Oncology, Institute of Industrial Ecological Sciences, University of Occupational and Environmental Health, Japan, 1-1 Iseigaoka, Yahatanishi-ku, Kitakyushu, Fukuoka 807-8555, Japan*
[e] *Faculty of Hygienic Chemistry, School of Pharmaceutical Sciences, Kyushu University of Health and Welfare, 1714-1 Yoshino-cho, Nobeoka, Miyazaki 882-8508, Japan*
[f] *Department of Molecular Biology, School of Health Sciences, Kyorin University, 476 Miyashita-cho, Hachioji, Tokyo 192-8505, Japan*

ARTICLE INFO

Article history:
Received 26 October 2007
Received in revised form 12 May 2008
Accepted 24 May 2008
Available online 7 June 2008

Keywords:
Eisenia fetida
8-Hydroxydeoxyguanosine
Cadmium
Mutagenicity
Reactive oxygen species

ABSTRACT

Heavy metal pollution of soil causes biological problems, such as mutagenicity to living organisms, including human beings. However, few methods have been developed to assess metal mutagenicity in soil. To avoid metal mutagenicity, an adequate bio-monitoring method is required. In the present study, to determine if the analysis of oxidative DNA damage generated in the earthworm is a useful bio-monitoring method for soil mutagenicity, the accumulation of 8-hydroxydeoxyguanosine (8-OH-dG), a major form of oxidative DNA damage, in *Eisenia fetida* (Savigny, 1826) treated with cadmium chloride ($CdCl_2$) or nickel chloride ($NiCl_2$) was analyzed. *E. fetida* was treated with Cd (10 or 200 μg/g soil) or Ni (10 or 200 μg/g soil) for 1, 2, and 3 weeks or 3 months. After metal exposure, the metal concentration in *E. fetida* was analyzed by atomic absorption spectrometry and the 8-OH-dG accumulated in *E. fetida* was analyzed by HPLC analyses and immunohistochemistry. Atomic absorption spectrometry revealed that Cd, but not Ni, accumulated within *E. fetida*. The 8-OH-dG levels in the DNA of *E. fetida* treated with Cd for 3 months were significantly higher than those in control *E. fetida*. Moreover, immunohistochemical analyses revealed that positive signals for 8-OH-dG accumulation in seminal vesicles were detected only in *E. fetida* treated with 10 μg of Cd for 3 months. Although some points remain unresolved, a bio-monitoring system analyzing the DNA damage generated in the earthworm might be useful for the assessment of the mutagenicity of soil contaminated with various heavy metals, such as Cd.

1. Introduction

Heavy metal pollution of soil is widespread across the globe and has caused biological problems, leading to potential toxicity to living organisms. Recent research found that the atmospheric input of heavy metals to agricultural systems also significantly contributed to metal loading in soil [1]. These complicated pathways of contamination make it difficult to avoid exposure to metals existing in our surroundings.

To avoid metal toxicity, we should first understand the features of metals and assess metal toxicity. However, the methods used for the assessment are often not sensitive enough, because metals can be toxic below the technical detection limits. To overcome this limitation, many research efforts have been made to develop detection techniques or assessment methods for metal contamination of soil. Furthermore, the toxic action of metals sometimes depends on their metabolites generated in living organisms. Thus, adequate methods to assess metal toxicity are difficult to develop.

A bio-monitoring method would be appropriate to evaluate metal toxicity, because of its sensitivity and availability for unknown metabolites [2–4]. This approach is also somewhat limited, because it could be available only for a specific combination of a living organism with certain substances. Hence, it is important to find adequate living organisms as bio-monitors for each assessment.

Recent research has indicated that the earthworm is a candidate organism as a bio-monitor for soil contaminants, because it plays an important role in the soil macrofauna biomass. The species *Eisenia*

* Corresponding author. Tel.: +81 93 695 3206; fax: +81 93 695 3299.
E-mail address: t-hirano@env.kitakyu-u.ac.jp (T. Hirano).

1383-5718/$ – see front matter © 2008 Elsevier B.V. All rights reserved.
doi:10.1016/j.mrgentox.2008.05.011

fetida (Savigny, 1826) is most commonly used in ecotoxicology as a useful bio-monitor for soil [5]. In particular, this species' proximity to the soil contaminants is a merit for the analysis [6,7].

Metal-induced mutagenicity is a serious problem for the diversity of living organisms and human health. To prevent mutagenicity-associated diseases, we must understand the substances around us and avoid the environmental mutagens. Therefore, the evaluation of soil mutagenicity is very important, and direct analyses of DNA damage generated in living organisms may provide precise and useful information.

It is believed that 8-hydroxy-2′-deoxyguanosine (8-OH-dG), a major form of oxidative DNA damage, may have an important role in carcinogenesis, because it causes the GC to TA transversion type point mutation [8–10]. 8-OH-dG is constantly generated in DNA and the nucleotide by reactive oxygen species (ROS). We have studied the relationship between 8-OH-dG accumulation in DNA and health-related factors, such as smoking [11], chemical agents [12–18], X-rays [19], aging [20–22], and physical exercise [23]. Therefore, it is predicted that the accumulation level of 8-OH-dG in the DNA of *E. fetida* would directly reflect the soil mutagenicity.

Of note, some heavy metals are known to affect 8-OH-dG repair systems, leading to 8-OH-dG accumulation. Heavy metals such as arsenic (As) [18,24], cadmium (Cd) [14,18,25,26], chromate (Cr) [27,28], manganese (Mn) [29], and lead (Pb) [30] inhibit 8-OH-dG excision repair activity or down-regulate the expression of 8-oxoguanine DNA glycosylase 1 (OGG1), a major repair enzyme for 8-OH-dG. Among these metals, the effects of Cd on 8-OH-dG repair systems were well documented. In particular, it was found that Cd inhibited 8-OH-dG excision repair activity or 8-OH-dGTPase activity, leading to 8-OH-dG accumulation in DNA [14,18,26,31]. This inhibitory action of Cd on the DNA repair system might be involved in Cd carcinogenesis.

In the present study, we analyzed 8-OH-dG accumulated in the DNA of *E. fetida* exposed to heavy metals, to determine if a method using earthworms as a bio-monitor is useful for the assessment of soil mutagenicity. We employed Cd and Ni as test metals, because the carcinogenic potentials of Cd and Ni have been established for humans and animals [32,33], and these metals are known to generate 8-OH-dG in DNA [14,34–36].

2. Materials and methods

2.1. Earthworms and heavy metal exposure

The *E. fetida* used in this study, which we had employed in the previous work [37], was kindly provided by Dr. C.A. Edwards (Ohio State University). They were kept in a 20-L stainless steel tank at an ambient temperature of 24 °C on mold with skim milk as a food source until heavy metal exposure. We used scrapped mold as soil, which consisted of the core of corn, rice bran, and other components and had been used for mushroom cultivation (gift from Ikesue Toyotada Shoten, Mizumagun, Japan). Adult organisms with a body wet weight of around 100 mg were used. Three (for a short-term experiment) or six (for a long-term experiment) individuals were kept in a 600 mL glass container containing 50 g of soil with/without heavy metal. They were exposed to 10 or 200 μg heavy metal/g soil for 1, 2, and 3 weeks or 10 μg heavy metal/g soil for 3 months (Fig. 1).

2.2. Atomic absorption spectrometry

The earthworm's body was cut into four rough segments: head region (S1), anterior body region (S2), posterior body region (S3), and tail region (S4). They were weighed under wet conditions and quickly frozen at −80 °C. The concentrations of heavy metals in each segment were determined using standard atomic absorption spectrometry. Each segment of *E. fetida* was transferred into a 100 mL kjeldahl flask and digested with a mixture of 5 mL nitric acid and 0.5 mL sulfuric acid. The flask was gently heated on a hot plate in a fume cupboard until only a few drops of clear liquid remained. After filtration, the samples were brought up to 10 mL with 0.1N nitric acid. This sample was analyzed by atomic absorption spectroscopy, with a Hitachi Model 180-80 spectrometer equipped with a graphite atomizer (Hitachi, Tokyo, Japan). The metal concentration was calculated from absorbance *versus* concentration curves prepared for each run of specimens. The metal concentration was expressed as micrograms per gram of body wet weight.

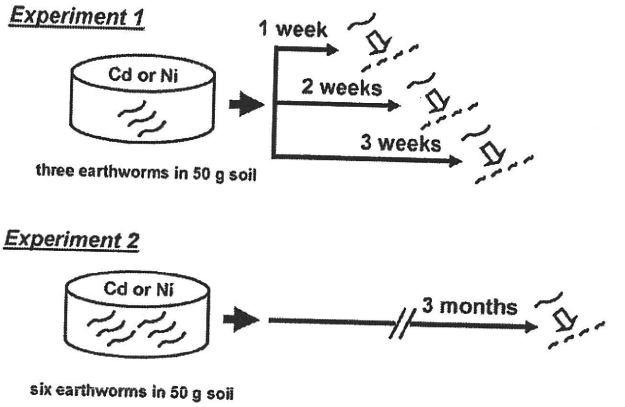

Fig. 1. Experimental design. Experiment 1 was a short-term exposure of *E. fetida* to $CdCl_2$ or $NiCl_2$. Metals (0, 0.5, or 10 mg as Cd or Ni) were added into 50 g soil per 600 mL glass container. After 0-, 1-, 2- and 3-week exposures, *E. fetida* were cut into four rough segments. We kept a total of 45 *E. fetida* (15 glass containers; 3 *E. fetida* per container). Experiment 2 was a long-term exposure of *E. fetida* to $CdCl_2$ or $NiCl_2$. Metals (0 or 0.5 mg as Cd or Ni) were added into 50 g soil per 600 mL glass container. After a 3-month exposure, *E. fetida* were cut into four rough segments. We kept a total of 54 *E. fetida* (9 glass containers; 6 *E. fetida* per container).

2.3. Quantitative analyses of 8-OH-dG levels

The 8-OH-dG levels in the S1 region of each earthworm (3-month experiment) were measured. The assay was described previously [40]. Briefly, DNA from the earthworms was isolated by the sodium iodide method, using a DNA Extraction WB Kit (Wako Pure Chemical Industries, Ltd., Japan). For homogenization, a lysis solution containing 1 mM desferal (deferoxamine mesylate, Sigma Chemical Co. MO, USA) was used. The isolated DNA was digested with nuclease P1 (Yamasa Corp., Choshi, Japan) and alkaline phosphatase (Roche Diagnosis GmbH, Mannheim, Germany) to obtain a deoxynucleoside mixture. The solution was filtered with an Ultrafree-Probind filter (Millipore, Bedford, MA) and was injected into a high-performance liquid chromatography (HPLC) column (Shiseido Capcell Pak C18 MG) equipped with an electrochemical detector (ECD) (ECD-300, Eicom Co., Kyoto, Japan). The 8-OH-dG value in the DNA was expressed as the percentage of the control value.

2.4. Immunohistochemistry

Samples were fixed in Bouin's solution for 3 h in ice. After fixation, they were cut into the four rough segments as described above, immersed in 90% ethanol for 24 h to remove the picric acid, dehydrated, and embedded in paraffin. These embedded samples were sagittally sectioned at 5 μm, mounted on glass slides coated with poly-L-lysine, and subjected to either hematoxylin/eosin (HE) or immunohistochemical (IHC) staining. The avidin–biotin complex method [38] was used to detect 8-OH-dG. We used the monoclonal antibody N45.1 (Nikken SEIL, Shizuoka, Japan), which was raised against 8-OH-dG, as the first antibody and biotin-labeled goat anti-mouse IgG serum (Vector Laboratories, Inc., Burlingame, California), and streptavidin–alkaline phosphatase complex (Vector Laboratories, Inc., Burlingame, California) diluted 1:100 [39]. The substrate for alkaline phosphatase (red) was obtained from the DAKO New Fuchsin Substrate System (DAKO, Copenhagen). For negative staining, a 2% bovine serum albumin solution was used instead of the first antibody. HE or IHC staining specimens were observed by Olympus BX50 System microscopy (Olympus, Tokyo, Japan).

2.5. Statistical analysis

Values obtained in the present study were calculated to the means ± S.D. The statistical significance was calculated using the Student *t*-test. Probability values less than 0.05 were considered to indicate significant differences.

3. Results

3.1. Body wet weights of E. fetida

All *E. fetida* used in the present study were weighed under wet conditions (Fig. 2). The body wet weights of *E. fetida* treated with 200 μg Cd/g soil for 2 weeks were significantly lower (49.5% of

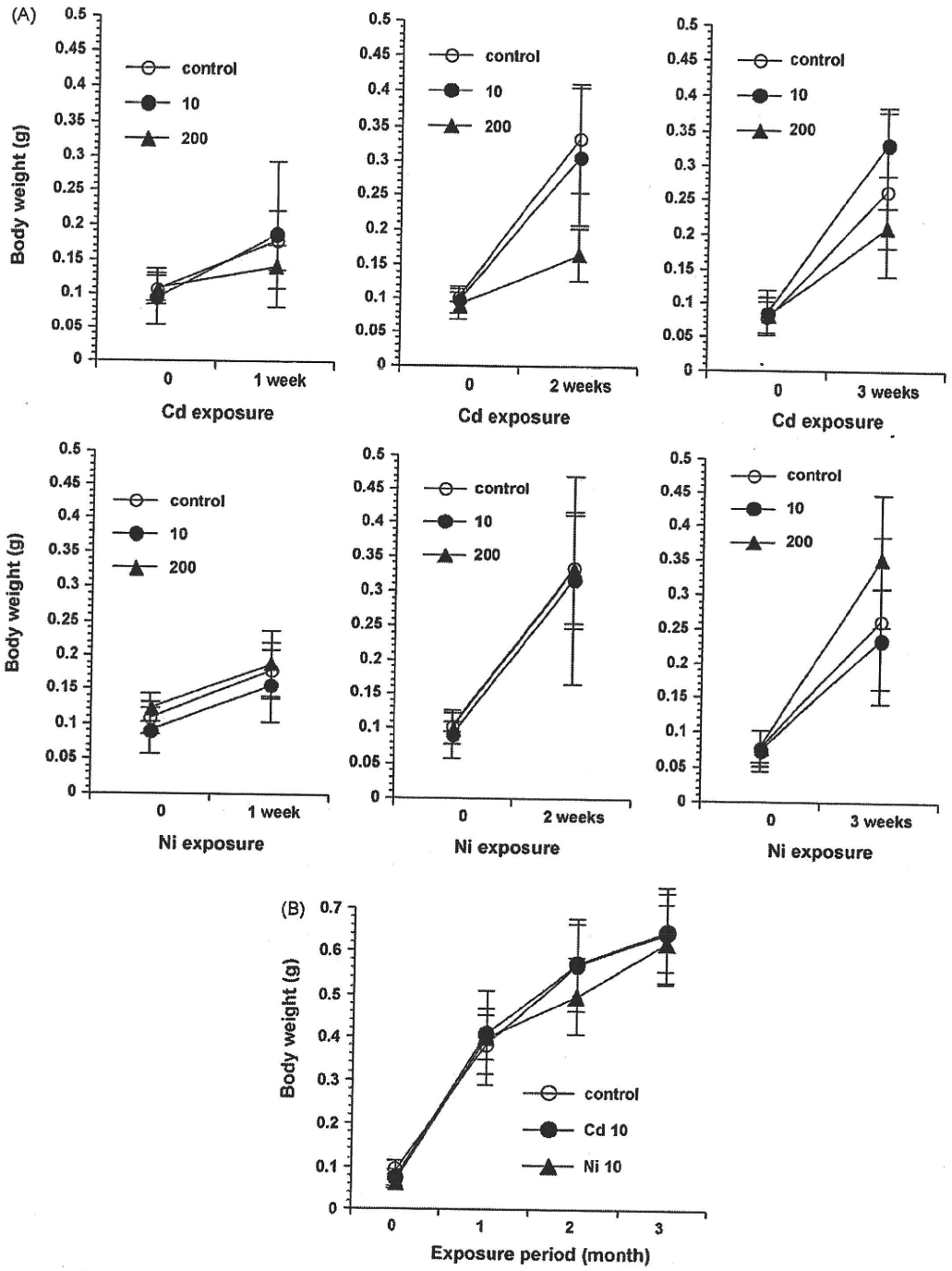

Fig. 2. All *E. fetida* were weighed under wet conditions in the short-term (A) and the long-term (B) experiments. Each data point represents the mean of six *E. fetida*. The treatment of *E. fetida* with 200 μg Cd/g soil resulted in body weight loss, suggesting Cd-induced growth inhibition. In the long-term experiment, each data point represents the mean of 16 *E. fetida*, and no significant differences between any groups were observed.

control) than those of all other 2-week exposure individuals (*versus* control, $p < 0.001$; *versus* 10 μg Cd/g soil treatment group, $p < 0.01$; *versus* 10 μg Ni/g soil treatment group, $p < 0.05$; *versus* 200 μg Ni/g soil treatment group, $p < 0.005$). The body wet weights of *E. fetida* treated with 200 μg Cd/g soil for 3 weeks were significantly lower than those of some other 3-week exposure individuals (*versus* 10 μg Cd/g soil treatment group, $p < 0.01$; *versus* 200 μg Ni/g soil treatment group, $p < 0.01$). However, no growth inhibition was observed in *E. fetida* treated with 10 μg Cd/g soil, even in a 3-month exposure. No inhibitory effects were also observed with the Ni exposure. All earthworms were alive during the experiment.

3.2. Cd and Ni concentrations in *E. fetida*

The Cd and Ni concentrations in *E. fetida* were analyzed using atomic absorption spectrometry. In a short-term experiment, Cd accumulated in the head (S1) and anterior body (S2) regions at an early stage (1 week) and in all segments at a later stage (2 and 3

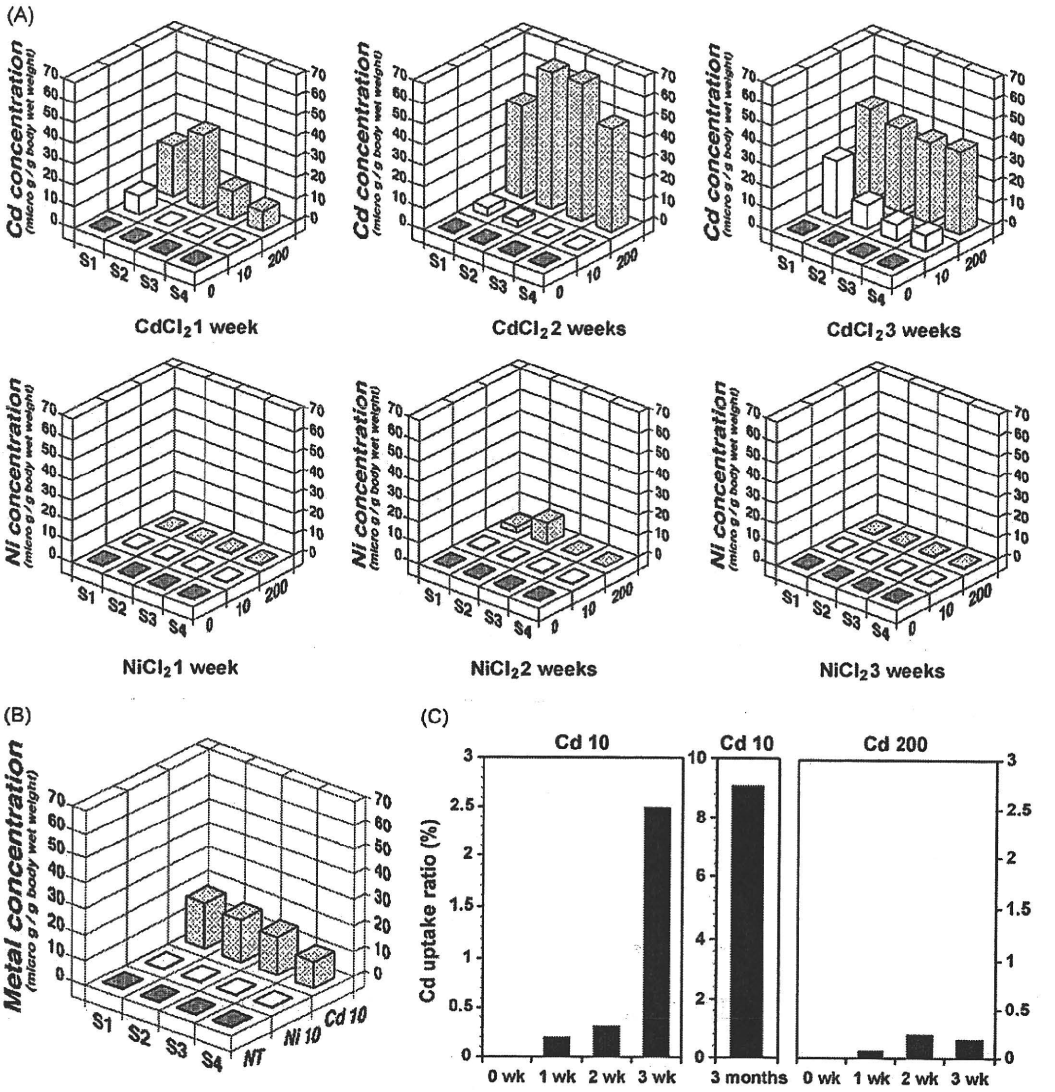

Fig. 3. Heavy metal accumulation in *E. fetida* in the short-term (A) and the long-term (B) experiments. Each data point represents the mean of three individuals. Heavy metal concentrations were measured by atomic absorption spectrometry, and are expressed as micrograms per gram of body wet weight. The percentage ratio of the uptake of Cd within 50 g soil by all *E. fetida* per container was calculated and shown (C).

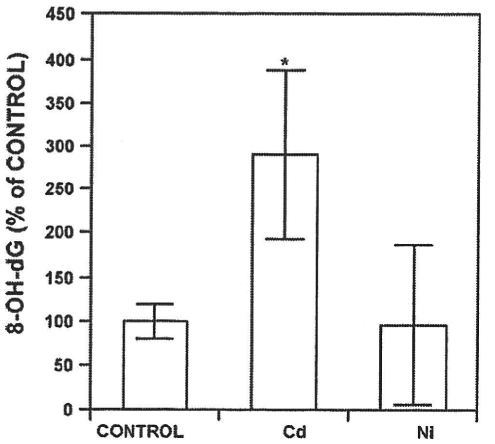

weeks) (Fig. 3A). To the contrary, Ni accumulation was not observed during this experiment, except for one individual data set (200 μg Ni/g soil, 2 weeks). In a long-term experiment, accumulation of Cd, not Ni, was detected in all segments (Fig. 3B). To determine how much the earthworms clean up the soil, the Cd uptake ratio by *E. fetida* was calculated. *E. fetida* took up at most ~2.5% of the Cd in 50 g soil in a short-term experiment and ~9% of the Cd in 50 g soil in a long-term experiment (Fig. 3C).

3.3. Accumulation levels of 8-OH-dG in the earthworm DNA

The 8-OH-dG levels in the DNA of earthworms treated with $CdCl_2$ for 3 months were significantly higher than those in control

Fig. 4. The 8-OH-dG levels in DNA from the S1 region of earthworms (3-month experiment) were analyzed by HPLC equipped with electrochemical detection. The values were expressed as % of control value. Mean values ± S.D., $n = 5$. Significant differences from the control group and Ni-treated group: $^*p < 0.005$ *vs.* control group, $p < 0.05$ versus Ni-treated group.

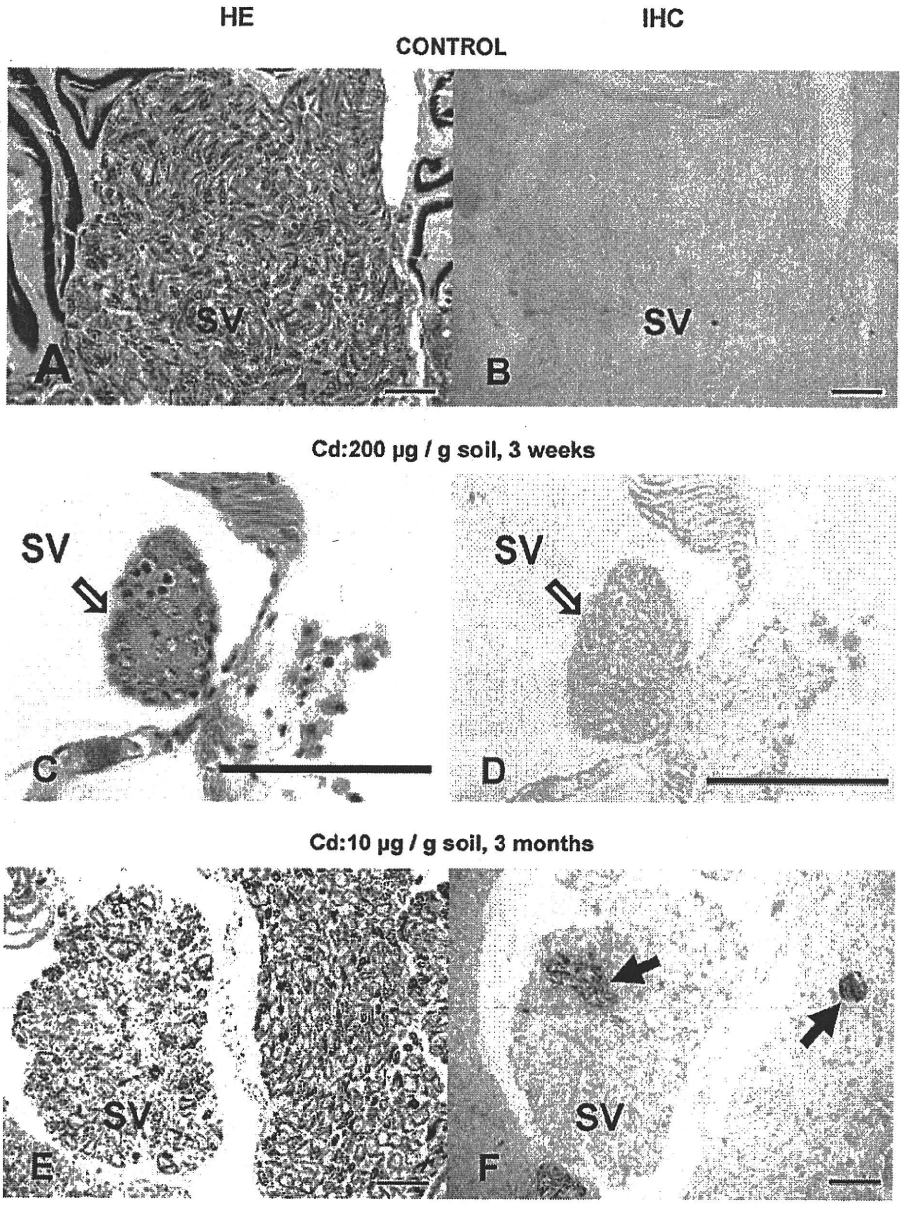

Fig. 5. Immunohistochemical analyses of 8-OH-dG accumulation in the seminal vesicles of *E. fetida* (S1) treated with Cd (200 μg/g soil, 3 weeks; HE (C), IHC (D)), and Cd (10 μg/g soil, 3 months; HE (E), IHC (F)). Controls: (A) and (B). Positive signals for 8-OH-dG accumulation in the seminal vesicles were detected only in *E. fetida* treated with Cd (10 μg/g soil) for 3 months. HE stained section and IHC stained section are in several serial sections. Arrowheads (black) show positive signals in seminal vesicles. SV: seminal vesicles. All scale bars are 100 μm.

earthworms or in earthworms treated with $NiCl_2$ (Fig. 4). These results are compatible with those from the immunohistochemical analyses, in which positive signals for 8-OH-dG in seminal vesicles (in S1 region) were clearly detected.

3.4. Immunohistochemical detection of 8-OH-dG accumulation in *E. fetida*

Positive signals in seminal vesicles were detected only in *E. fetida* treated with 10 μg Cd for 3 months (Fig. 5). Besides these signals, no significant difference was detected in the other metal-treated specimens in comparison to the control. In addition, 8-OH-dG accumulation was detected in the gut epithelial layers in almost all specimens (data not shown). Since ROS are easily generated by non-specific environmental factors, it is reasonable that 8-OH-dG was present in almost all gut epithelial layers.

4. Discussion

Among the many kinds of living organisms in soil, the earthworm is a most useful organism for the evaluation of metal contamination in soil, because significant positive correlations have been found between the metal concentrations in the earthworm and the soil Cd, copper, lead and zinc concentrations [41]. This evidence prompted us to verify the utility of the earthworm as a bio-monitor.

In the present study, we observed Cd accumulation in the anterior segment of the earthworm *E. fetida* at an early stage and

gradually almost equally in all four segments, suggesting that Cd might be accumulated in multiple organs (Fig. 3). It is well known that one biological effect of some heavy metals, such as Cd accumulation, in organisms is growth inhibition [42]. In the present study, the body wet weight of *E. fetida* decreased to 49.5% of the control by 200 μg Cd/g soil exposure. Thus, the growth inhibition observed in the present study indicated that the *E. fetida* actually suffered from the Cd accumulated in their organs. On the other hand, little Ni accumulation and no inhibitory effects of Ni exposure on *E. fetida* growth were observed.

We observed increased 8-OH-dG levels in DNA of the S1 region of Cd-treated earthworms in comparison to the other groups of earthworms (control or Ni-treated earthworms) (Fig. 4). In addition, the positive signals in the seminal vesicles were clearly detected only in *E. fetida* treated with 10 μg of Cd at 3 months (Fig. 5), although Cd accumulation was detected in all S1 segments, including the 200 μg Cd-exposed specimens, in which seminal vesicles were located. These findings seemed to be specific to long-term Cd exposure, and raised the question of why Cd treatment of *E. fetida* increased the 8-OH-dG accumulation only in that organ. One possible explanation for this question is the distribution of metal-binding proteins. On the other hand, we observed positive staining of 8-OH-dG in the gut epithelial layers in almost all samples. The metal absorption routes include the digestive system and the surface wall [43,44], but the main route is the digestive system. Since gut epithelial layers are frequently exposed to ROS, 8-OH-dG accumulation was constantly detected.

In mammals, the cysteine-rich metal-binding protein, metallothionein (MT), exists especially in the liver and kidney, and plays a key role in metal detoxification. However, mammalian testes and ventral prostate had either no induction or a reduced expression of the MT gene when the animals were exposed to Cd or some other MT-inducing agents [45,46]. MT is a ubiquitous metal-binding protein found in plants, invertebrates including earthworm, and mammals. Earthworm MT, which has two isoforms (MT-1 and MT-2), was also identified and cloned [47]. Recently, MT expression was detected in the intestinal region, chlorangogenous tissue, and gut of *Lumbricus rubellus* collected from an arsenic/copper-contaminated site [48]. Thus, MT expression plays a key role in Cd-induced toxicity or mutagenicity.

In the present study, positive signals for 8-OH-dG accumulation were detected in the seminal vesicles, which are considered as MT-poor organs. Therefore, it seems reasonable to speculate that a lower level of MT expression is involved in Cd-induced DNA damage accumulation. To address this speculation, the relationship between the localizations of Cd, MT, and 8-OH-dG accumulation should be clarified as a further study. Moreover, the seminal vesicles are located in S1, in which Cd accumulated from an early stage, suggesting that long-term exposure to Cd might also contribute to an increase in 8-OH-dG accumulation in seminal vesicles. Thus, it is reasonable to conclude that an increase in 8-OH-dG accumulation in seminal vesicles might reflect long-term exposure to Cd.

The carcinogenic potentials of Cd and Ni have been established for humans and experimental animals [32,33]. In addition, both Cd and Ni are known to increase 8-OH-dG generation in human and animal DNA [14,34–36]. Hence, we employed Cd and Ni as test metals. In the present study, we observed a high level of Cd accumulation and little Ni accumulation in *E. fetida*, accompanied with an increase in 8-OH-dG accumulation in the seminal vesicles of Cd-exposed *E. fetida*. Based on these results, it is reasonable to conclude that the increase in 8-OH-dG accumulation is due to Cd accumulation and incomplete metal detoxification in the seminal vesicles of *E. fetida*. In addition, Cd reportedly inhibited 8-OH-dGTPase activity, but Ni did not [31]. This evidence might also explain the differences in the levels of 8-OH-dG accumulation.

Taken together, our results demonstrate the possible utility of a bio-monitoring method for assessing soil mutagenicity, by using earthworms as bio-monitors and measuring the oxidative DNA damage generated in the earthworm. Immunohistochemical analyses are useful to detect the locations of 8-OH-dG accumulation, but unlike HPLC analyses, they are not quantitative. Therefore, a method using both HPLC and immunohistochemical analyses is recommended. However, many points remain unresolved. For example, this method could be reliable only for bio-accumulated metals, such as Cd, but not for non-bio-accumulated metals, such as Ni, even if they generate 8-OH-dG. To establish a bio-monitoring method using earthworms for soil mutagenicity, further studies will be required.

Acknowledgements

We would like to express our thanks to Dr. C.A. Edwards (Ohio State University) for providing the *E. fetida* and Ikesue Toyotada Shoten (Mizuma-gun, Japan) for the supply of scrapped mold. This work was supported by a grant from The Foundation for Earth Environment.

References

[1] M. Vidovic, A. Sadibasic, S. Cupic, M. Lausevic, Cd and Zn in atmospheric deposit, soil, wheat, and milk, Environ. Res. 97 (2005) 26–31.
[2] M. Harnly, S. Seidel, P. Rojas, R. Fornes, P. Flessel, D. Smith, R. Kreutzer, L. Goldman, Biological monitoring for mercury within a community with soil and fish contamination, Environ. Health Perspect. 105 (1997) 424–429.
[3] F. Regoli, S. Gorbi, D. Fattorini, S. Tedesco, A. Notti, N. Machella, R. Bocchetti, M. Benedetti, F. Piva, Use of the land snail *Helix aspersa* as sentinel organism for monitoring ecotoxicologic effects of urban pollution: an integrated approach, Environ. Health Perspect. 114 (2006) 63–69.
[4] S. Citterio, R. Aina, M. Labra, A. Chiani, P. Fumagalli, S. Sgorbati, A. Santagostino, Soil genotoxicity assessment: a new strategy based on biomolecular tools and plant bioindicators, Environ. Sci. Technol. 36 (2002) 2748–2753.
[5] F. Brulle, G. Mitta, C. Coquerelle, D. Vieau, S. Lemiere, A. Leprêtre, F. Vandenbulcke, Cloning and real-time PCR testing of 14 potential biomarkers in *Eisenia fetida* following cadmium exposure, Environ. Sci. Technol. 40 (2006) 2844–2850.
[6] A.J. Reinecke, S.A. Reinecke, Earthworm as test organisms in ecotoxicological assessment of toxicant impacts on ecosystems, in: C.A. Edwards (Ed.), Earthworm Ecology, CRC Press LLC, Boca Baton, FL, 2004, pp. 299–320.
[7] N.T.T.M. Steenbergen, F. Iaccino, M. De Winkel, L. Reijnders, W.J.G.M. Peijnenburg, Development of a biotic ligand model and a regression model predicting acute copper toxicity to the earthworm *Aporrectodea caliginosa*, Environ. Sci. Technol. 39 (2005) 5694–5702.
[8] M.L. Wood, M. Dizdaroglu, E. Gajewski, J.M. Essigmann, Mechanistic studies of ionizing radiation and oxidative mutagenesis: genetic effects of a single 8-hydroxyguanine (7-hydro-8-oxoguanine) residue inserted at a unique site in a viral genome, Biochemistry 29 (1990) 7024–7032.
[9] S. Shibutani, M. Takeshita, A.P. Grollman, Insertion of specific bases during DNA synthesis past the oxidation-damaged base 8-OH-dG, Nature 349 (1991) 431–434.
[10] K.C. Cheng, D.S. Cahill, H. Kasai, S. Nishimura, L.A. Loeb, 8-Hydroxyguanine, an abundant form of oxidative DNA damage, causes G→T and A→C substitutions, J. Biol. Chem. 267 (1992) 166–172.
[11] S. Asami, T. Hirano, R. Yamaguchi, Y. Tomioka, H. Itoh, H. Kasai, Increase of a type of oxidative DNA damage, 8-hydroxyguanine, and its repair activity in human leukocytes by cigarette smoking, Cancer Res. 56 (1996) 2546–2549.
[12] R. Yamaguchi, T. Hirano, S. Asami, A. Sugita, H. Kasai, Increase in the 8-hydroxyguanine repair activity in the rat kidney after the administration of a renal carcinogen, ferric nitrilotriacetate, Environ. Health Perspect. 104 (1996) 651–653.
[13] R. Yamaguchi, T. Hirano, S. Asami, K.M. Chung, A. Sugita, H. Kasai, Increased 8-hydroxyguanine levels in DNA and its repair activity in rat kidney after administration of a renal carcinogen, ferric nitrilotriacetate, Carcinogenesis 17 (1996) 2419–2422.
[14] T. Hirano, Y. Yamaguchi, H. Kasai, Inhibition of 8-hydroxyguanine repair in testes after administration of cadmium chloride to GSH-depleted rats, Toxicol. Appl. Pharmacol. 147 (1997) 9–14.
[15] R. Yamaguchi, T. Hirano, Y. Ootsuyama, S. Asami, Y. Tsurudome, S. Fukada, H. Yamato, T. Tsuda, I. Tanaka, H. Kasai, Increased 8-hydroxyguanine in DNA and its repair activity in hamster and rat lung after intratracheal instillation of crocidolite asbestos, Jpn. J. Cancer Res. 90 (1999) 505–509.
[16] Y. Tsurudome, T. Hirano, H. Yamato, I. Tanaka, M. Sagai, H. Hirano, N. Nagata, H. Itoh, H. Kasai, Changes in levels of 8-hydroxyguanine in DNA, its repair and

OGG1 mRNA in rat lungs after intratracheal administration of diesel exhaust particles, Carcinogenesis 20 (1999) 1573–1576.
[17] T. Hirano, K. Higashi, A. Sakai, Y. Tsurudome, Y. Ootsuyama, R. Kido, H. Kasai, Analyses of oxidative DNA damage and its repair activity in the livers of 3′-methyl-4-dimethylaminoazobenzene-treated rodents, Jpn. J. Cancer Res. 91 (2000) 681–685.
[18] N. Mei, N. Kunugita, T. Hirano, H. Kasai, Acute arsenite-induced 8-hydroxyguanine is associated with inhibition of repair activity in cultured human cells, Biochem. Biophys. Res. Commun. 297 (2002) 924–930.
[19] N. Mei, K. Tamae, N. Kunugita, T. Hirano, H. Kasai, Analysis of 8-hydroxydeoxyguanosine 5′-monophosphate (8-OH-dGMP) as a reliable marker of cellular oxidative DNA damage after gamma-irradiation, Environ. Mol. Mutagen. 41 (2003) 332–338.
[20] T. Hirano, Y. Yamaguchi, H. Hirano, H. Kasai, Age-associated change of 8-hydroxyguanine repair activity in cultured human fibroblasts, Biochem. Biophys. Res. Commun. 214 (1995) 1157–1162.
[21] T. Hirano, R. Yamaguchi, S. Asami, N. Iwamoto, H. Kasai, 8-Hydroxyguanine levels in nuclear DNA and its repair activity in rat organs associated with age, J. Gerontol. A51 (1996) B303–B307.
[22] Y. Tsurudome, T. Hirano, K. Hirata, A. Higure, N. Nagata, K. Takahashi, H. Itoh, H. Kasai, Age associated increase of 8-hydroxydeoxyguanosine in human colorectal tissue DNA, J. Gerontol. 56A (2001) B483–485.
[23] S. Asami, T. Hirano, R. Yamaguchi, Y. Tsurudome, H. Itoh, H. Kasai, Effects of forced and spontaneous exercise on 8-hydroxydeoxyguanosine levels in rat organs, Biochem. Biophys. Res. Commun. 243 (1998) 678–682.
[24] T. Hirano, K. Kawai, Y. Ootsuyama, H. Kasai, Fragmentation of the DNA repair enzyme, OGG1, in mouse nonparenchymal liver cells by arsenic compounds, Genes Environ. 28 (2006) 62–67.
[25] R.J. Potts, R.D. Watkin, B.A. Hart, Cadmium exposure down-regulates 8-oxoguanine DNA glycosylase expression in rat lung and alveolar epithelial cells, Toxicology 184 (2003) 189–202.
[26] C.K. Youn, S.H. Kim, D.Y. Lee, S.H. Song, I.Y. Chang, J.W. Hyun, M.H. Chung, H.J. You, Cadmium down-regulates human OGG1 through suppression of Sp1 activity, J. Biol. Chem. 280 (2005) 25185–25195.
[27] N.J. Hodges, J.K. Chipman, Down-regulation of the DNA-repair endonuclease 8-oxo-guanine DNA glycosylase 1 (hOGG1) by sodium dichromate in cultured human A549 lung carcinoma cells, Carcinogenesis 23 (2002) 55–60.
[28] A.J. Lee, N.J. Hodges, J.K. Chipman, Interindividual variability in response to sodium dichromate-induced oxidative DNA damage: role of the $Ser^{326}Cys$ polymorphism in the DNA-repair protein of 8-oxo-7, 8-dihydro-2′-deoxyguanosine DNA glycosylase 1, Cancer Epidemiol. Biomarkers Prev. 14 (2005) 497–505.
[29] V. Sava, D. Mosqouera, S. Song, F. Cardozo-Pelaez, J.R. Sánchez-Ramos, Effects of melanin and manganese on DNA damage and repair in PC12-derived neurons, Free Rad. Biol. Med. 36 (2004) 1144–1154.
[30] J. Sanchez-Ramos, E. Overvik, B.N. Ames, A marker of oxyradical-mediated DNA damage (oxo8dG) is increased in nigrostriatum of Parkinson's disease brain, Neurodegeneration (Exp. Neurol.) 3 (1994) 197–204.
[31] K. Bialkowski, A. Bialkowska, K.S. Kasprzak, Cadmium(II), unlike nickel(II), inhibits 8-OH-dGTPase activity and increases 8-OH-dG level in DNA of the rat testis, a target organ for cadmium(II) carcinogenesis, Carcinogenesis 20 (1999) 1621–1624.
[32] IARC, Chromium, Nickel, Welding. IARC Monographs, vol. 49, IARC, Lyon, 1990.
[33] IARC, Beryllium, Cadmium, Mercury and Exposures in the Glass Manufacturing Industry. IARC Monographs, vol. 58, IARC, Lyon, 1993.
[34] H. Dalley, A. Hartwig, Induction and repair inhibition of oxidative DNA damage by nickel(II) and cadmium(II) in mammalian cells, Carcinogenesis 18 (1997) 1021–1026.
[35] H. Merzenich, A. Hartwig, W. Ahrens, D. Beyersmann, R. Schlepegrell, M. Scholze, J. Timm, K.H. Jöckel, Biomonitoring on carcinogenic metals and oxidative DNA damage in a cross-sectional study, Cancer Epidemiol. Biomark. Prev. 10 (2001) 515–522.
[36] J.G. Hengstler, U. Bolm-Audorff, A. Faldum, K. Janssen, M. Reifenrath, W. Götte, D. Jung, O. Mayer-Popken, J. Fuchs, S. Gebhard, H.G. Bienfait, K. Schlink, C. Dietrich, D. Faust, B. Epe, F. Oesch, Occupational exposure to heavy metals: DNA damage induction and DNA repair inhibition prove co-exposures to cadmium, cobalt and lead as more dangerous than hitherto expected, Carcinogenesis 24 (2003) 63–73.
[37] T. Suzuki, M. Honda, S. Matsumoto, S.R. Stüzenbaum, S. Gamou, Valosine-containing proteins (VCP) in an annelid: identification of a novel spermatogenesis related factor, GENE 362 (2005) 11–18.
[38] S.M. Hsu, L. Raine, H. Fanger, A comparative study of the peroxidase–anti-peroxidase method and an avidin–biotin complex method for studying the polypeptide hormones with radioimmunoassay antibodies, Am. J. Clin. Pathol. 75 (1981) 734–738.
[39] Y. Hattori, C. Nishigori, T. Tanaka, K. uchida, O. Nikaido, T. Osawa, H. Hiai, S. Imamura, S. Toyokuni, 8-Hydroxy-2′-deoxyguanosine is increased in epidermal cells of hairless mice after chronic ultraviolet B exposure, J. Invest. Dermatol. 107 (1997) 733–737.
[40] K. Kawai, Y.S. Li, H. Kasai, Accurate measurement of 8-OH-dG and 8-OH-Gua in mouse DNA, urine and serum: effects of X-ray irradiation, Genes Environ. 29 (2007) 107–114.
[41] J.E. Morgan, A.J. Morgan, Earthworms as biological monitors of cadmium, copper, lead and zinc in metalliferous soils, Environ. Pollut. 54 (1988) 123–138.
[42] M.G. Burgos, C. Winters, S.R. Stürzenbaum, P.F. Randerson, P. Kille, A.J. Morgan, Cu and Cd effects on the earthworm *Lumbricus rubellus* in the laboratory: multivariate statistical analysis of relationships between exposure, biomarkers, and ecologically relevant parameters, Environ. Sci. Technol. 39 (2005) 1757–1763.
[43] J.K. Saxe, C.A. Impellitteri, W.J. Peijnenburg, H.E. Allen, Novel model describing trace metal concentrations in the earthworm, *Eisenia andrei*, Environ. Sci. Technol. 35 (2001) 4522–4529.
[44] M.G. Vijver, H.T. Wolterbeek, J.P. Vink, C.A. van Gestel, Surface adsorption of metals onto the earthworm *Lumbricus rubellus* and the isopod *Porcellio scaber* is negligible compared to absorption in the body, Sci. Total Environ. 340 (2005) 271–280.
[45] T.P. Coogan, N. Shiraishi, M.P. Waalkes, Minimal basal activity and lack of metal-induced activation of the metallothionein gene correlates with lobe-specific sensitivity to the carcinogenic effects of cadmium in the rat prostate, Toxicol. Appl. Pharmacol. 132 (1995) 164–173.
[46] G. Xu, G. Zhou, T. Jin, T. Zhou, S. Hammarstrom, A. Bergh, G. Nordberg, Apoptosis and p53 gene expression in male reproductive tissues of cadmium exposed rats, Biometals 12 (1999) 131–139.
[47] S.R. Stürzenbaum, P. Kille, A.J. Morgan, The identification, cloning and characterization of earthworm metallothionein, FEBS Lett. 431 (1998) 437–442.
[48] C.J. Langdon, C. Winters, S.R. Stürzenbaum, A.J. Morgan, J.M. Charnock, A.A. Meharg, T.G. Piearce, P.H. Lee, K.T. Semple, Ligand arsenic complexation and immunoperoxidase detection of metallothionein in the earthworm *Lumbricus rubellus* inhabiting arsenic-rich soil, Environ. Sci. Technol. 39 (2005) 2042–2048.

DOI 10.1002/mnfr.200600122 Mol. Nutr. Food Res. 2008, 52, 360–369

Research Article

Functional analyses of neutrophil-like differentiated cell lines under a hyperglycemic condition

Tomoko Oya-Ito[1,2], Hirotaka Naitou[1], Shuichi Masuda[1], Naohide Kinae[1,2] and Norio Ohashi[1,2]

[1] Graduate School of Nutritional and Environmental Sciences, University of Shizuoka, Shizuoka, Japan
[2] COE program in the 21st Century and Global COE program, University of Shizuoka, Shizuoka, Japan

Diabetic patients are prone to severe bacterial infections. The functional alterations of neutrophils by hyperglycemia are thought to be partially responsible for such infections. In this study, we investigated the functional changes of neutrophil-like differentiated cell lines (dHL-60, dTHP-1, and dNB-4) by treatment with 5.5 mM, 11 mM, or 35 mM of glucose. In dHL-60 cells, the incubation with high glucose (35 mM) resulted in the enhancement of cell aggregation, the suppression of cellular fragility, the induction of reactive-oxygen species (ROS) production by phorbol myristate acetate (PMA) stimulation, and the impairment of phagocytosis. In dTHP-1 cells, the treatment with higher glucose generated the suppression of cellular fragility and extremely impaired phagocytosis (by 35 mM), and induced ROS production due to PMA stimulation (by 11 mM). Furthermore, the higher glucose exposure to dNB-4 cells enlarged intracellular vacuoles (by 35 mM) and induced ROS production due to PMA stimulation (by 11 mM). Since the ROS generation of those cells was enhanced only after PMA stimulation under the higher glucose conditions, glucose may have a priming effect rather than a triggering effect. These extraordinary sensitivities caused by the higher glucose treatments may reflect the dysfunction or overactivation of neutrophils.

Keywords: Diabetes / High glucose condition / Neutrophil-like differentiated human myeloid leukemia cell lines / Phagocytosis / Reactive oxygen species production

Received: July 28, 2006; revised: July 31, 2007; accepted: October 5, 2007

1 Introduction

Severe bacterial infections are common in diabetic patients with hyperglycemia [1]. Neutrophils serve as a first defense line against pathogenic bacteria. The bactericidal activity of neutrophil is primarily due to oxidative pathway. By the assembly of enzymatic components (known as NADPH oxidase) segregated into the cytoplasm and plasma membrane of resting polymorphonuclear leukocyte (PMN) [2, 3], the bactericidal oxidants such as superoxide anion are produced from the activated neutrophils. Previous studies have shown that PMN in diabetic patients have impaired chemotaxis, phagocytosis, and oxidative and bactericidal activities [4–9]. A possible explanation for the impairment of PMN phagocytosis activities in diabetics is the influence due to the elevation of serum glucose concentration [10] and advanced glycation end-products (AGEs) [11, 12]. The short-term treatment (30 min) of PMN from healthy donors with high glucose concentration reduced the cellular respiratory burst [13]. Moreover, neutrophils from poorly controlled diabetics have impaired the ability of superoxide generation in the response to formyl-Met-Leu-Phe (fMLP) but not phorbol myristate acetate (PMA), and phospholipase D activity is decreased in the response to fMLP [10]. However, the detailed mechanisms of functional abnormalities of neutrophils under the hyperglycemic condition remain elusive. In our preliminary *ex vivo* experiment for 8 h or more, it was hard to examine the neutrophil function, because most neutrophils prepared from healthy humans rapidly died due to apoptosis.

Human promyelocytic leukemia cell lines, HL-60, THP-1, and NB-4, have been extensively used for several

Correspondence: Professor Norio Ohashi, 52-1 Yada, Shizuoka 422-8526, Japan
E-mail: ohashi@u-shizuoka-ken.ac.jp
Fax: +81-54-264-5793

Abbreviations: AGEs, advanced glycation end-products; **ATRA**, All-*trans* retinoic acid; **dHL-60**, differentiated HL-60; **dNB-4**, differentiated NB-4; **dTHP-1**, differentiated THP-1; **GM-CSF**, granulocyte-macrophage colony-stimulating factor; **NBT**, nitroblue tetrazolium; **PKC**, protein kinase C; **PMA**, phorbol myristate acetate; **PMN**, polymorphonuclear neutrophil; **ROS**, reactive-oxygen species

researches, *e. g.* the cellular differentiation and proliferation [14, 15], in worldwide laboratories. All-*trans* retinoic acid (ATRA) is well known as an inducer for cell differentiation, in particular it promotes the granulocytic maturation of human promyelocytic leukemia HL-60 cells [16–18]. The ATRA-differentiated HL-60 cells acquire the ability of reduction of nitroblue tetrazolium (NBT) [16–21], increase the tissue transglutaminase expression [19], modulate the proto-oncogene expression [20], induce the cell-surface expression of the Mac-i antigen [22], and up-regulate the protein kinase activity [21, 23]. NB-4 is a cell line derived from an acute promyelocytic leukemia patient and its differentiation can be induced by ATRA as well. Fleck *et al.* [24] have assessed the morphological changes such as cell spreading and flattening during the differentiation of HL-60 and NB-4 with ATRA toward a neutrophil-like phenotype by scanning electron microscopy. The cell-cycle progression of human monocytic cell line THP-1 is regulated by ATRA through the G1/S phase [25]. The mRNA expression of retinoic acid receptor (RAR) alpha of THP-1 cells is induced by granulocyte macrophage colony-stimulating factor (GM-CSF), and the NBT reducing activity of THP-1 cells is increased by the synergistic effect of ATRA and GM-CSF [26]. The expression of CD11b antigen (a cell surface marker of differentiation) on HL-60, NB-4 and THP-1 cells is increased by ATRA, as is phagocytosis activity [24, 25]. Thus, the HL-60 and NB-4 cells differentiated with ATRA, and the THP-1 cells differentiated with ATRA and GM-CSF are probably available for analysis of neutrophil-like function by treatment with high glucose for 24 h or more as hyperglycemic models. The aim of this study is to characterize the functional changes of those three differentiated cell lines under hyperglycemic conditions.

2 Materials and methods

2.1 Cell cultures

Three human leukemia cell lines (HL-60, NB-4 and THP-1) were maintained in RPMI 1640 medium including 11 mM glucose (a cell-maintaining medium, Iwaki, Japan) supplemented with 10% fetal calf bovine serum (FCS) at 37°C in 5% CO_2 atmosphere.

2.2 Cell differentiation

Cells were harvested during exponential growth and seeded at a density of 2×10^5 cells/ mL. The HL-60 and NB-4 cells were differentiated with 1 μM ATRA for 2 days in the cell-maintaining medium including 11 mM glucose (dHL-60 and dNB-4). For the differentiation of THP-1, the cells were cultured with 1 μM ATRA and 1 ng/mL GM-CSF for 2 days in the cell-maintaining medium (dTHP-1). The differentiation of those cells was monitored by NBT reducing assay as described later.

2.3 Treatment of cells with the different concentration of glucose

The differentiated or non-differentiated cells cultured in the cell-maintaining medium including 11 mM glucose were washed with PBS before experiments. For the mimicry of physiological conditions, the medium with addition of 5.5 mM glucose in glucose-free RPMI 1640 (Invitrogen, California, USA) was used. The cells (3×10^5 cells/mL of each) were incubated with a 5.5 mM glucose-containing medium (physiologic concentration), a 11 mM glucose-containing medium (*in vitro* cell-maintaining concentration), a 35 mM glucose-containing medium (addition of 24 mM glucose in cell-maintaining medium, high concentration), or a 24 mM mannitol-11 mM glucose-containing medium (addition of 24 mM mannitol in the cell-maintaining medium to rule out osmotic stress) for up to 4 days.

2.4 Cellular morphology, viability, vacuolization, and fragility

To characterize cellular morphology, the cells were prepared on glass slides by centrifugation using a Cytospin at 50 × g for 2 min, and the slides were air-dried, fixed in methanol and stained with Diff-Quik (Dade Behring, Illinois, USA) and were observed at a magnification of 1000 × under a light microscope. To examine cell viability, the number of living and dead cells in the cultures was determined by trypan blue dye exclusion under a phase contrast microscope. The ratio of living/dead cells was estimated as cell viability. For the observation of cellular vacuolization, the cells were stimulated with 10 ng/mL of PMA for 10 min, cytospined, fixed, and stained with Diff-Quik. The vacuolated cells were observed under a light microscope. For analysis of cellular fragility, the cells were stimulated with 10 ng/mL of PMA for 10 min, cytospined, fixed, and stained with Diff-Quik, and the number of cells was counted under a light microscope. The cells on the slide lack fragile cells, which were destroyed physically by cytospining. The percentage of cellular fragility was determined by the following equation: % of cellular fragility = [destroyed-Diff-Quik-stained cells/total-Diff-Quik-stained cells] × 100. Each individual experiment was repeated at least three times.

2.5 Cell aggregation assay

The number of aggregated cells and total cells was counted under a phase contrast microscope. The percentage of cells in aggregates was determined by the following equation: %

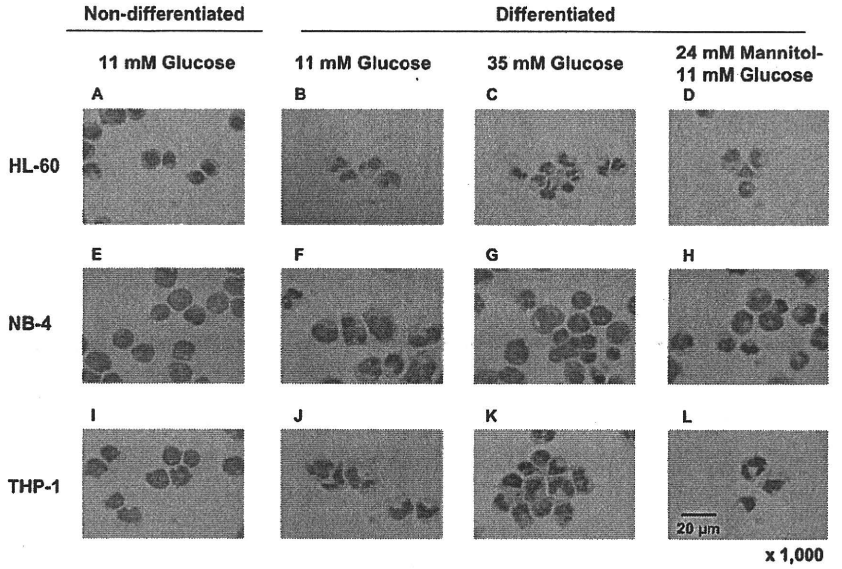

Figure 1. Morphological characteristics of non-differentiated and differentiated HL-60, NB-4, and THP-1 cells cultured with the different concentration of glucose. The cell lines were maintained in RPMI 1640 medium containing 11 mM glucose (A: HL-60, E: NB-4, I: THP-1). Differentiated cells were prepared by treatment with 1 μM ATRA for 2 days (dHL-60: B–D and dNB-4: F–H), or with 1 μM ATRA and 1 ng/mL GM-CSF for 2 days (dTHP-1: J–L). The differentiated cells were further cultured for 4 days with 11 mM glucose (B, F, and J), 35 mM glucose (C, G, and K), and 24 mM mannitol-11 mM glucose (D, H, and L). All cells used were stained with Diff-Quik.

of cells in aggregates = [aggregated cells/total cells] × 100. Each individual experiment was repeated at least three times.

2.6 NBT reducing assay

The cells ($0.4-1 \times 10^6$) were centrifuged at $700 \times g$ for 5 min, suspended with 1 mL PBS containing 2 mg/mL of NBT and 10 ng/mL of PMA, and incubated for 60 min at 37°C. The reaction was terminated by the addition of 0.4 mL of 2 N HCl and kept cooling on ice for 30 min. After centrifugation at $700 \times g$ for 5 min, the formazan deposits in the pellets were dissolved with 1 mL of DMSO, and the absorbance at 540 nm was measured. Each individual experiment was repeated at least four times. In some experiments, after NBT treatments with or without stimulation of PMA, the formazan-stained or non-stained cells were directly observed under a phase contrast microscope.

2.7 Phagocytosis of yeast by differentiated cells

Yeast particles (*Saccharomyces cerevisiae*; Sigma-Aldrich, Missouri, USA) were added to the suspension of differentiated cells in HBSS containing 5% fresh human serum and left in contact with the cells for 30 min at 37°C [27]. The final concentrations of yeast and differentiated cells were 6.25×10^7 particles/mL and 2.5×10^6 cells/mL, respectively. After centrifugation, the cell pellets were stained with Ziehl's carbolfuchsin solution (Sigma-Aldrich). The yeast particles outside the cells were stained red, and the yeast particles completely ingested by the cells were protected from taking up the stain. The cells containing unstained yeast particles were considered as cells capable of phagocytosis.

2.8 Statistical analysis

Data are presented as mean ± SD. Differences between mean values were determined by ANOVA. Differences with $p < 0.05$ were considered statistically significant.

3 Results

Three human myeloid leukemia cell lines, HL-60, NB-4, and THP-1, which were differentiated with ATRA alone or with ATRA and GM-CSF in the cell-maintaining medium containing 11 mM glucose for 2 days, showed PMN-like cell morphologies and the ratio of cytoplasm to nucleus was increased (Figs. 1A, B, E, F, I, and J). These differentiated cells, dHL-60, dNB-4, and dTHP-1, acquired NBT reducing abilities and their CD11b expressions were increased by FACS analysis (data not shown). By further treatment of the differentiated cells with 35 mM glucose or 24 mM manni-

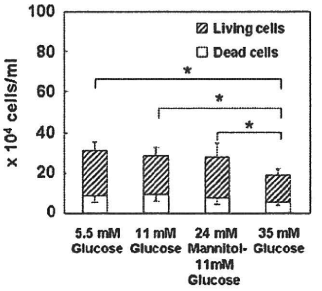

Figure 2. Effect of glucose on the cell concentration of dHL-60. After differentiation, the cells were exposed to the conditions of 5.5 mM glucose, 11 mM glucose, 35 mM glucose, and 24 mM mannitol-11 mM glucose for 4 days. The number of living and dead cells was determined by trypan blue dye exclusion under a phase contrast microscope and the sum is shown as the cell concentration (cells/mL). Data are mean ± SD from three or more independent experiments performed in quadruplicate. *, $p < 0.005$.

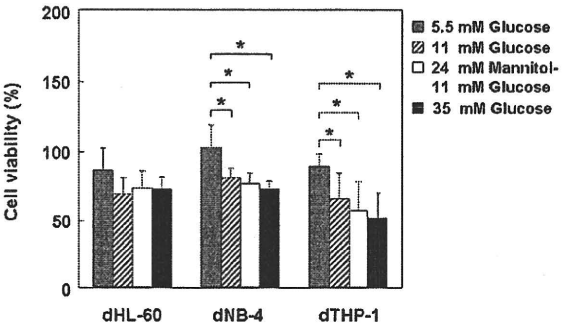

Figure 3. Effect of glucose on the cell viabilities of dHL-60, dNB-4, and dTHP-1. After differentiation, the cells were exposed to 5.5 mM glucose, 11 mM glucose, 35 mM glucose, and 24 mM mannitol-11 mM glucose for 4 days. The numbers of living and dead cells were determined by trypan blue exclusion under the phase contrast microscope. The ratio of living/dead cells was estimated as "cell viability". Data are mean ± SD from three or more independent experiments performed in quadruplicate. *, $p < 0.005$.

tol-11 mM glucose for 4 days, there were little morphological differences between those glucose- and mannitol-treated cells (Figs. 1C, D, G, H, K, and L), and the cellular fragility under high glucose condition with 35 mM was reduced in the dHL-60 and dTHP-1 cells after PMA stimulation as described later.

In healthy human blood, the glucose concentration is in the range of 5–6 mM (*in vivo*), but the established cell lines such as HL-60, THP-1, and NB-4 were usually maintained with 11 mM glucose in RPMI 1640 medium (*in vitro*). Therefore, we first examined the effects of three different concentration of glucose, 5.5 mM (physiologic concentration), 11 mM (*in vitro* cell-maintaining concentration), and 35 mM (high concentration), on the differentiated cells. In the cell concentration of dHL-60 (Fig. 2), no significant difference was found among the differentiated cells treated with 5.5 mM glucose, 11 mM glucose, and 24 mM mannitol-11 mM glucose during the cultures for 4 days, whereas the cell concentration in dHL-60 treated with 35 mM glucose decreased approximately up to 65% of those in cells treated with the other concentration of glucose ($p < 0.005$). No effect of dNB-4 and dTHP-1 cells by treatment with 35 mM glucose for 4 days on the cell concentration was found (data not shown). Cell viabilities (a ratio of living/dead cells) of dNB-4 and dTHP-1 cultured for 4 days with 5.5 mM glucose were significantly increased when compared with those of the other concentrations of glucose (Fig. 3, $p < 0.05$), but there was no significant difference among the viability of dHL-60 cells treated with any different concentration of glucose. These results suggest that the culture for 4 days with higher glucose concentration (up to 35 mM) did not induce mortal damages such as cytotoxicity in those cell lines.

By treatment of dHL-60 with 35 mM glucose for 4 days, the cellular aggregation was increased (Fig. 4). The mean

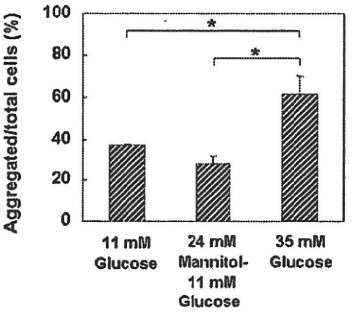

Figure 4. Effect of glucose on the cellular aggregation of dHL-60. The cells were exposed to 11 mM glucose, 35 mM glucose, and 24 mM mannitol-11 mM glucose for 4 days. The numbers of aggregated and total cells were counted under microscope and the percentage was determined. Data are mean ± SD from three to six replicate cultures. Each individual experiment was repeated a minimum of three times. *, $p < 0.05$.

value of aggregation under the high glucose condition with 35 mM was estimated to be 62.1 ± 8.4%, while the corresponding values under the conditions with 11 mM glucose and 24 mM mannitol-11 mM glucose were 37.3 ± 0.3% and 27.8 ± 4.0%, respectively. Statistical analysis revealed that the high glucose condition with 35 mM significantly enhanced the cellular aggregation ($p < 0.05$). Further PMA stimulation did not affect the cell aggregation of dHL-60 cells (data not shown). The dNB-4 and dTHP-1 cells showed no differences in the cell aggregation among treatments with 35 mM glucose, 11 mM glucose, and 24 mM mannitol-11 mM glucose. However, additional PMA stimulation of dNB-4 and dTHP-1 cells treated with 35 mM glucose promoted the cellular aggregations (data not shown).

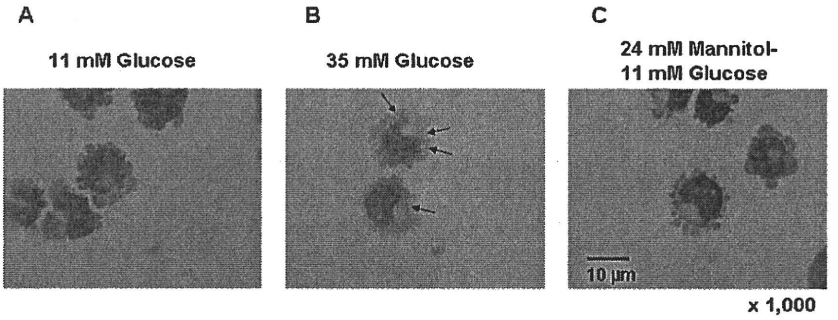

Figure 5. Effect of glucose on the intracellular vacuolation of dNB-4. The cells were exposed to 11 mM glucose (A), 35 mM glucose (B), and 24 mM mannitol-11 mM glucose (C) for 4 days. After stimulation with 10 ng/mL of PMA for 10 min, the exposed cells were stained with Diff-Quik. Arrows show cytoplasmic vacuoles.

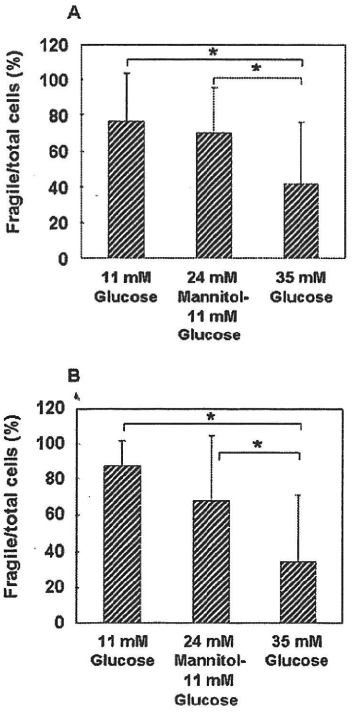

Figure 6. Effect of glucose on the cellular fragility of dHL-60 (A) and dTHP-1 (B). The cells were exposed to 11 mM glucose, 24 mM mannitol-11 mM glucose, and 35 mM glucose for 4 days. After stimulation with 10 ng/mL of PMA for 10 min, the exposed cells were stained with Diff-Quik and counted. The percentage of the cellular fragility was estimated by equation in Section 2. Data are mean ± SD from three to six replicate cultures. Each individual experiment was repeated a minimum of three times. *, $p < 0.02$.

By PMA stimulation after incubation with 35 mM glucose for 4 days (arrows in Fig. 5), the intracellular vacuolation of dNB-4 cells was induced. An equal amount of 24 mM mannitol-11 mM glucose did not enlarge vacuoles, suggesting that osmotic pressure did not affect such vacuolation. When the dNB-4 cells were not stimulated with PMA, no difference of vacuolation was observed among the cells treated with 35 mM glucose, 11 mM glucose, and 24 mM mannitol-11 mM glucose.

Since many fragile cells of dHL-60 and dTHP-1 were observed by PMA stimulation, the effect of glucose on the cellular fragility after PMA stimulation was examined. In dHL-60 and dTHP-1 cells, the fraction of fragile cells was reduced in the cultures with 35 mM glucose compared to the cultures with 11 mM glucose and 24 mM mannitol-11 mM glucose for 4 days (Fig. 6, $p < 0.02$). In both dHL-60 and dTHP-1 cells, the fragilities due to osmotic shock were not observed as shown in treatment with 24 mM mannitol-11 mM glucose. The suppressions of cellular fragility by the cultures with 35 mM glucose were observed only when the cells were triggered with PMA.

Production of reactive-oxygen species (ROS), especially superoxide anion, was determined by NBT reducing assay in cells cultured with different concentration of glucose. In all three differentiated cells cultured with 11 mM glucose for 24 h, the superoxide production by PMA stimulation were markedly increased compared to the culture with 5.5 mM glucose (Fig. 7A, $p < 0.0002$). In dHL-60 cultured with 35 mM glucose for 24 h, the superoxide production of the cells by PMA stimulation was1.5-fold increased compared to the cultures with 11 mM as well as 5.5 mM glucose (Fig. 7B, $p < 0.0001$). However, the short-term treatment for 5 h with 35 mM glucose did not affect the superoxide generation of dHL-60 (Fig. 7C). The superoxide generation of dNB-4 and dTHP-1 cells in culture with 35 mM glucose for 24 h, 11 mM glucose, and 24 mM mannitol-11 mM glucose was significantly increased compared with 5.5 mM glucose (Fig. 7B, $p < 0.0001$). The induction of superoxide production was not observed when these differentiated cells were cultured with concentrations of glucose without the PMA stimulation (Fig. 7A, and the microscopic observation of dHL-60 cells treated with 35 mM glucose as a representative in Fig. 7D).

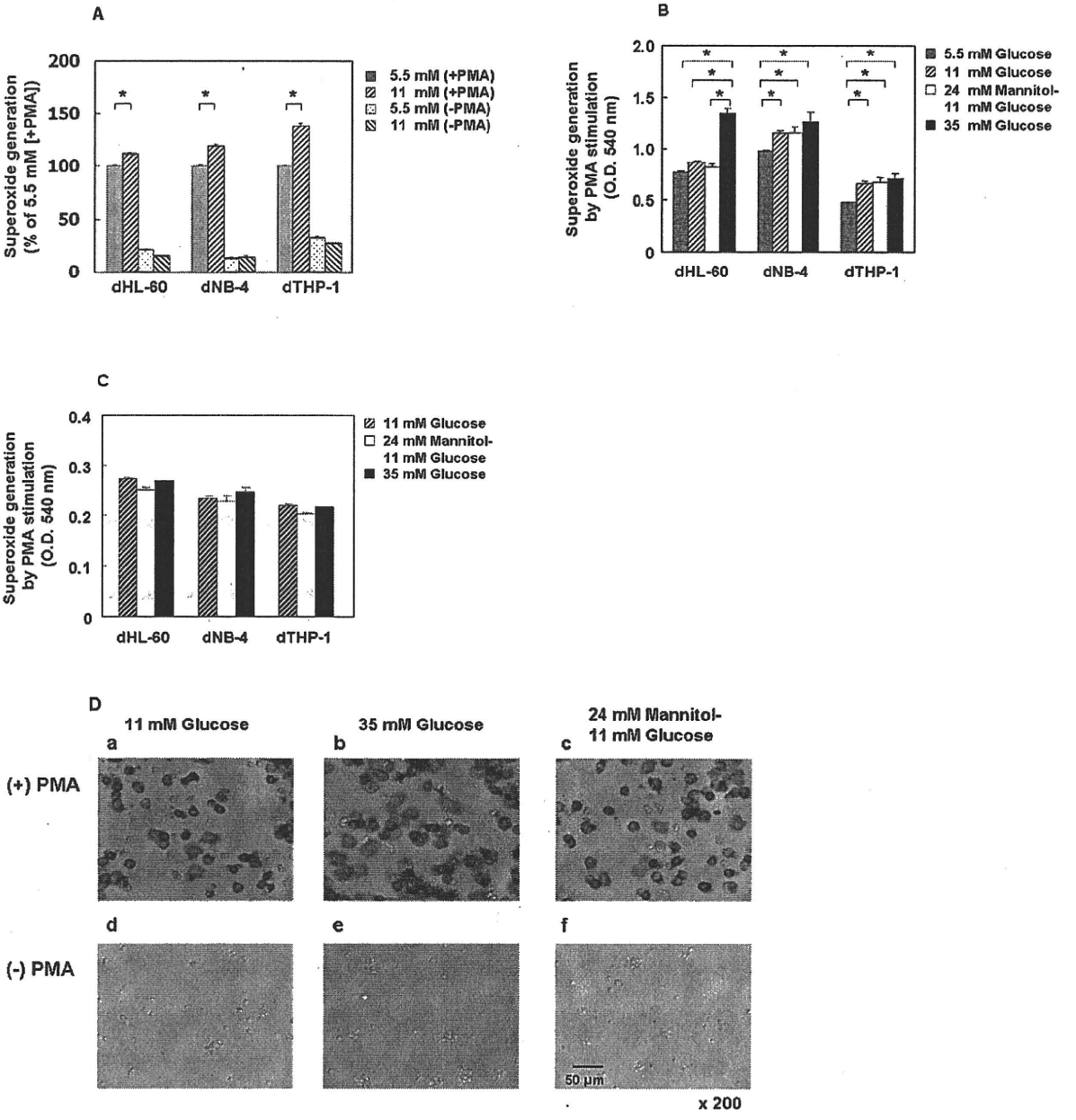

Figure 7. Effect of glucose on the superoxide generation of dHL-60, dNB-4, and dTHP-1 with or without PMA stimulation. The superoxide generation of differentiated and glucose-treated cells was evaluated by NBT reduction assay. Data are mean ± SD from three or more independent experiments. (A) Superoxide generation of the PMA-stimulated or non-stimulated cells after the culture for 24 h with 5.5 mM glucose (shaded bar) and 11 mM glucose (hatched bar). *, $p < 0.0002$. (B) Superoxide generation of the PMA-stimulated cells after the culture for 24 h with 5.5 mM glucose (shaded bar), 11 mM glucose (hatched bar), 24 mM mannitol-11 mM glucose (open bar), and 35 mM glucose (solid black bar). *, $p < 0.0001$. (C) Superoxide generation of the PMA-stimulated cells after the culture for 5 h (short-term) with 11 mM glucose, 24 mM mannitol-11 mM glucose, and 35 mM glucose, no significance was observed. (D) Morphological characteristics of the PMA-stimulated and non-stimulated dHL-60 cells cultured for 24 h with 11 mM glucose (a and d), 35 mM glucose (b and e), 24 mM mannitol-11 mM glucose (c and f). The blue-colored dHL-60 observed under the phase contrast microscope shows the formazan-deposited cells due to superoxide generation after PMA stimulation.

